



OPEN ACCESS

EDITED BY

Geórgenes Hilário Cavalcante,
Federal University of Alagoas, Brazil

REVIEWED BY

Kyra St.Pierre,
University of British Columbia, Canada
Phoebe Zito,
University of New Orleans,
United States

*CORRESPONDENCE

Dorina Murgulet
dorina.murgulet@tamucc.edu

SPECIALTY SECTION

This article was submitted to
Coastal Ocean Processes,
a section of the journal
Frontiers in Marine Science

RECEIVED 04 June 2022

ACCEPTED 12 August 2022

PUBLISHED 08 September 2022

CITATION

Douglas AR, Murgulet D, Greige M,
Das K, Felix JD and Abdulla HA (2022)
Organic matter composition and
inorganic nitrogen response to
Hurricane Harvey's negative storm
surge in Corpus Christi Bay, Texas.
Front. Mar. Sci. 9:961206.
doi: 10.3389/fmars.2022.961206

COPYRIGHT

© 2022 Douglas, Murgulet, Greige, Das,
Felix and Abdulla. This is an open-
access article distributed under the
terms of the [Creative Commons
Attribution License \(CC BY\)](https://creativecommons.org/licenses/by/4.0/). The use,
distribution or reproduction in other
forums is permitted, provided the
original author(s) and the copyright
owner(s) are credited and that the
original publication in this journal is
cited, in accordance with accepted
academic practice. No use,
distribution or reproduction is
permitted which does not comply with
these terms.

Organic matter composition and inorganic nitrogen response to Hurricane Harvey's negative storm surge in Corpus Christi Bay, Texas

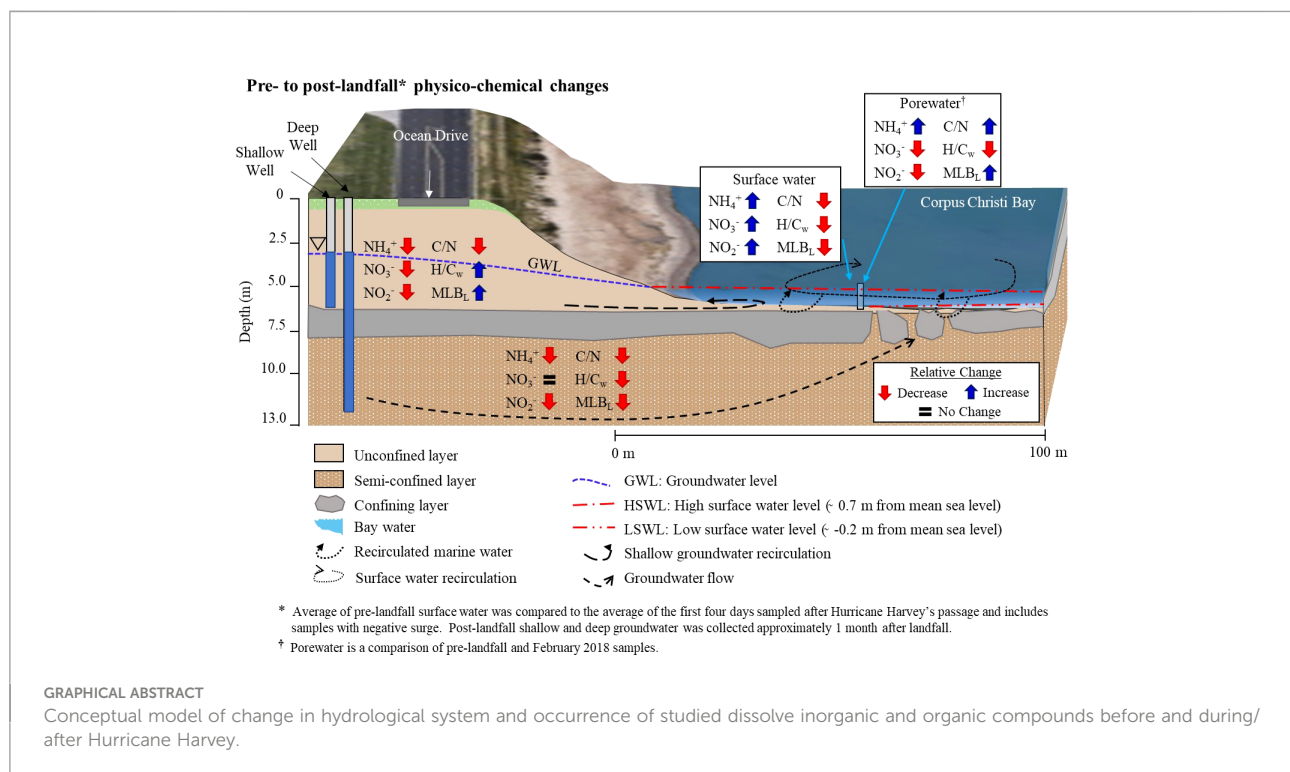
Audrey R. Douglas^{1,2}, Dorina Murgulet^{1*}, Megan Greige¹,
Kousik Das¹, J. David Felix¹ and Hussain A. Abdulla¹

¹Center for Water Supply Studies, Department of Physical and Environmental Science, Texas A&M University-Corpus Christi, Corpus Christi, TX, United States, ²Harte Research Institute for Gulf of Mexico Studies, Texas A&M University-Corpus Christi, Corpus Christi, TX, United States

Extreme weather events, such as tropical storms and hurricanes, are known to deliver large amounts of freshwater (surface runoff) and associated inorganic and organic nutrients to estuaries and the coastal ocean, affecting water quality and nutrient budgets. However, while Hurricane Harvey produced an unprecedented 1,000-year flood event in 2017 that inundated areas north of the landfall, like the Houston/Galveston region (Texas, United States), the impact on the Corpus Christi area, south of the landfall, was an intermittent negative surge (~0.5 m below mean sea level (MSL)), caused by the southerly direction of winds and limited freshwater inflows. With the use of pre- and post-landfall surface-water, porewater, and groundwater nutrient measurements and dissolved organic matter (DOM) molecular characterization analyses, this study assessed the influence of negative storm surge on groundwater-surface water interactions and nutrient composition. Within 2 weeks following the first landfall, the forms and inputs of inorganic and organic nutrients fluctuated significantly nearshore Corpus Christi Bay. Sudden drops in sea level were correlated with pulses of NH_4^+ and disproportionately more dissolved organic carbon (DOC) than dissolved organic nitrogen (DON), likely from a carbon-rich groundwater or benthic source with slightly lower labile characteristics. Recovery to MSL drove higher proportions of nitrogenous DOM and lower dissolved inorganic nitrogen (DIN) inputs. An increased presence of sulfurized DOM derived from anaerobic microbial processing of organic matter mineralization in marine sediments post-landfall was facilitated by enhanced groundwater inputs and flushing of porewater due to considerable drops in sea level and steepening hydraulic gradients toward the coast. The induced pulses of higher groundwater advective fluxes are also hypothesized to have intermittently enhanced flushing of anoxic DIN and biodegraded DOM from porewater and groundwater and suggested that dynamic hurricane-induced negative surge events affect net nutrient budgets in estuarine and coastal seas.

KEYWORDS

extreme event, hydrologic changes, nitrogen sources, estuarine chemistry, Orbitrap-MS, groundwater-surface water interactions



1 Introduction

Extreme hydroclimatic events, such as hurricanes, droughts, and floods, have been predicted to increase in frequency and intensity due to climate change (Webster et al., 2005). These changes are expected to reflect on the delivery of freshwater, nutrients, sediments, and dissolved organic matter (DOM) to estuaries, thus greatly influencing the biogeochemical cycling and ecological productivity in estuaries (Riera et al., 2000; Montagna et al., 2012). The estuarine nitrogen cycle is disrupted by extreme storm events like hurricanes through increased loading of nutrients from runoff, which may trigger eutrophication and algal bloom propagation (Paerl et al., 1998; Mallin et al., 1999; Shelton, 2009). However, only in recent years has the impact of storm events on organic matter cycling and composition become the focus of research in riverine (Raymond and Saiers, 2010; Lu and Liu, 2019) and estuarine systems (Letourneau and Medeiros, 2019).

With its important contribution of carbon (C) and carbon-bound nutrients, such as nitrogen (N), phosphorus (P), and sulfur (S) to estuaries, DOM plays an important role in the biogeochemistry and ecological functioning of coastal environments (Findlay and Sinsabaugh, 2004; Carlson and Hansell, 2015). Studies indicate that DOM affects the solubility (Chiou et al., 1986), bioavailability (Akkanen et al., 2004; Ksionzek et al., 2018), and reactivity (Opsahl and Benner, 1997) of nutrients, trace metals, and contaminants in aquatic environments. Transformations of DOM at the land–ocean

boundaries, like estuaries, play a key role in the biochemical transformations of nutrients; thus, further studies are necessary.

There are several sources of autochthonous and allochthonous DOM in the estuarine environments (Lee et al., 2020). Autochthonous sources include *in situ* marine production by primary producers, exudation of aquatic plants, and aquatic plant degradation (Carlson and Hansell, 2015). Allochthonous sources are associated with terrestrial inputs *via* soil and plant matter degradation (Bauer and Bianchi, 2011) and anthropogenic contributions from industry, agricultural runoff, and domestic sewage (Griffith and Raymond, 2011). As expected, terrestrial DOM sources dominate where freshwater inputs are significant, whereas estuarine-derived DOM inputs are more dominant in low-flow estuaries (Sipler and Bronk, 2015; Santos et al., 2016). The source and degree of DOM biodegradation in estuarine and marine environments are reflected in the molecular characteristics. For instance, terrestrial DOM is characterized by more aromatic compounds and a greater CHO composition, due to the nature of terrestrial plant detritus (Bianchi and Bauer, 2011). In comparison, marine DOM is characterized by higher weighted averages of phosphorous (P) and nitrogen (N) heteroatoms and aliphatic compounds (Bianchi and Bauer, 2011). The quantity and forms of DOM influence estuarine ecology through changes in microbial community composition (Traving et al., 2017; D'Andrilli et al., 2019), with implications for seasonal changes in marine primary productivity. For instance, biotic and abiotic breakdown of terrestrially derived DOM from rivers to coastal

margins was found to contribute to coastal eutrophication (Duan et al., 2007; DeVilbiss et al., 2016). Thus, while the organic matter is a vital resource subsidy that supports ecosystem diversity (Savage et al., 2012), excess inputs of DOM can stimulate harmful algal blooms, especially during warm months and increased runoff from storms (Boyer et al., 2006).

Hydrologic processes control the transport path and the rate of terrestrial DOM transformation within a watershed and to coastal waters (Shang et al., 2018; Singh et al., 2019). Hydrologic perturbations such as those caused by extreme hydroclimatic events are expected to influence the quantity of DOM and inorganic nutrient inputs, composition, and degradation pathways in estuarine waters. These physical processes induce changes in temperature, pH, and salinity, among other hydrologic characteristics, which in turn have the ability to influence estuarine DOM bioavailability and transformations (Liu et al., 2019). Given the different sources and sinks for DOM converging in estuaries, including riverine inputs, flanking marshes, groundwater and benthic fluxes, atmospheric deposition, and oceanic waters (Hedges and Keil, 1999), these types of investigations are scarce and have proven challenging.

While recent studies have begun to assess changes in DOM after storm events, the focus has been on surface runoff caused by compounded storm surges and rain (Denis et al., 2017; Chen et al., 2019; Schafer et al., 2020; Gold-Bouchot et al., 2021). For many of these studies, storm surges and flooding were found to be the major source of terrestrial DOM to marine waters during storm events, normally as a result of increased precipitation and runoff (Inamdar et al., 2011; Chen et al., 2019; Lu and Liu, 2019). However, the 2017 Hurricanes Harvey (Goff et al., 2019) and Irma (So et al., 2019) caused abrupt drops in surface water levels, exposing long stretches of bay bottoms, a rare phenomenon called seaward or negative storm surge. This extreme change in water level is expected to affect hydraulic gradients and act as a pull of groundwater discharge offshore, particularly in shallow and microtidal embayments. These disturbances, however, have not been considered in evaluations of inorganic nutrient and organic matter inputs to coastal waters. This study evaluated changes in DOM composition and sourcing and inorganic nutrients as a function of the dynamic coupling of hydrological and estuarine physical and biogeochemical processes nearshore Corpus Christi Bay in response to the negative surge caused by Hurricane Harvey. It is expected that the short-term dynamic changes in the underlying physical processes in coastal estuarine areas control the chemical form, timing, and inputs of nutrients and DOM. The evaluation included a high-frequency daily sampling of nearshore Corpus Christi Bay following Hurricane Harvey and DOM molecular characterization (using ultrahigh-performance liquid chromatography (UPLC) coupled with mass spectrometry (MS)) and inorganic nutrient analyses in relation to physical changes. Statistical analyses were employed

to identify unique aspects of hurricane impacts on the chemical composition of bay water and its association with physical processes.

2 Methods

2.1 Study area

Samples were collected on the southern shore of Corpus Christi Bay at University Beach on Ward Island, near Texas A&M University-Corpus Christi (TAMU-CC; Figure 1). Corpus Christi Bay, a shallow primary bay (average depth of 3.4 m) in the Nueces Estuary, connects to the Gulf of Mexico through a pass in the barrier island and to the secondary bays, Nueces Bay and Oso Bay, where the rivers discharge (Figure 1B). Bay bottom sediments are comprised of fine sand and silt along the shoreline and mud toward the middle of the bay (Morton and Winker, 1979; Gardner et al., 2006). Ward Island is a remnant of the Nueces River and Oso Creek deltaic complex discharging into the bay. University Beach (Figure 1C) was constructed on the north shore of Ward Island in 2001 to restore the beach that once extended along the entire shoreline fronting the island. Terminal groins stabilize 366 m of the beach, and three detached breakwaters protect the beach from forces exerted on the shore.

The study area is mostly classified as semiarid, with average precipitation rates that vary between 81 cm year⁻¹, to the north, to 69 cm year⁻¹, to the south of the study location. Average evaporation rates range between 133 and 155 cm year⁻¹ (Behrens, 1966; TWDB, 2020). Typical average inflow rates to the Nueces Estuary are 10⁸ m³ year⁻¹ and change to a negative annual average (-10⁸ m³ year⁻¹) to the south in the Laguna Madre (Montagna et al., 2012). Low precipitation rates within the watersheds, water diversions, and river dams have resulted in absent to very limited freshwater inflows directly from the Nueces River (Murgulet et al., 2016). Oso Creek's contributions to Oso Bay and Corpus Christi Bay are largely dominated by permitted discharges (Sharma et al., 1999), including hypersaline inputs from the Barney M. Davis cooling reservoir (Bighash and Murgulet, 2015).

Corpus Christi Bay is located along the Texas Coastal Plain, which is a monoclinical belt structure, gently dipping (1.8–7.5 m per km) toward the Gulf of Mexico (Baker, 1979). The bay is in contact with the Chicot aquifer, which is part of the Gulf Coast Aquifer (GCA), a leaky artesian aquifer comprised of a complex of clays, silts, sands, and gravels (Ashworth and Hopkins, 1995). From well logs and electrical resistivity data collected as part of a previous study (Stearns, 2019), it is evident that the slightly deeper and semiconfined aquifer is in direct connection with the bay within 100 m offshore (Figure 1C). Similar conduits are expected to be present further offshore where dredging breached the shallow confining layer, thus explaining inputs of deeper groundwater further offshore during low water. Several recent

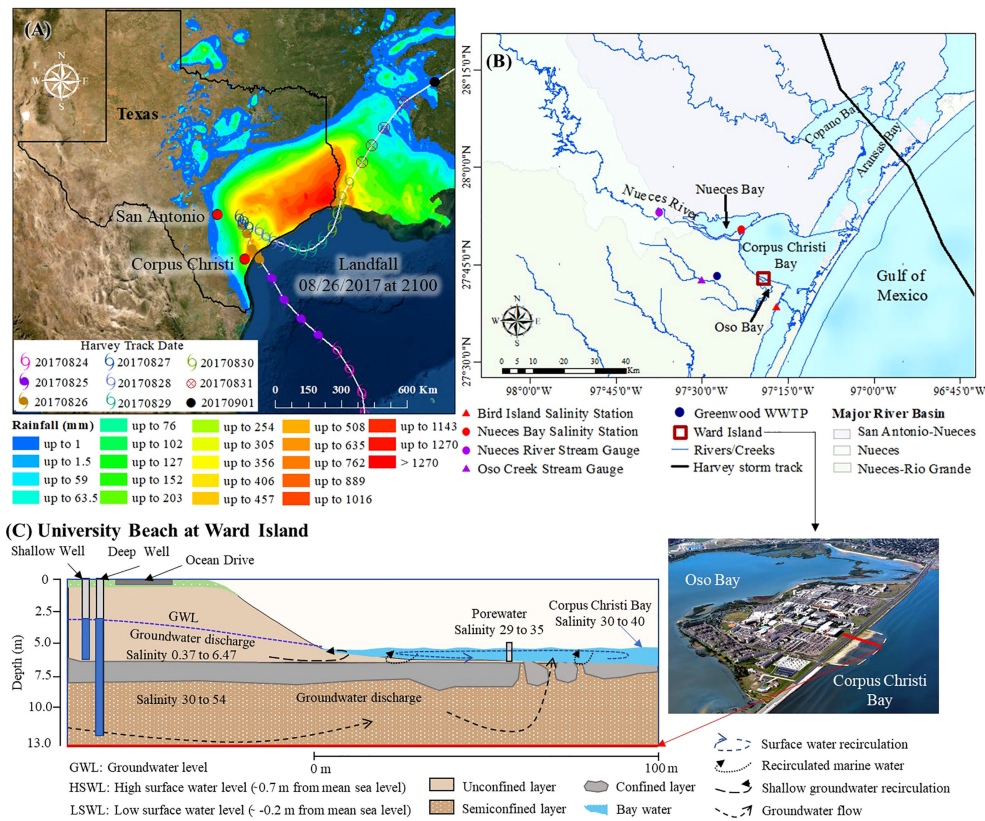


FIGURE 1

(A) The Hurricane Harvey path and Saffir–Simpson Hurricane Wind Scale categories (Blake and Zelinsky, 2018) and precipitation totals. (B) The geographic location of the study area with major river basins, stream gauges (Nueces River at Calallen, TX [08211500], and Oso Creek at Corpus Christi [08211520]), salinity stations (Nueces Bay [NUDE3, 043] and Bird Island [NPSBI, 171]), wastewater treatment plants (WWTP), and Harvey storm track shown. Samples were collected from the Texas A&M University–Corpus Christi beach on Ward Island (University Beach). (C) Overhead view of Ward Island (credit: TAMUCC MARCOM, CC BY-SA 4.0) showing the location of the sampling transect for the vertical cross-sectional representation of the study site with the sampling locations of groundwater and porewater shown. Surface water was collected in line with the groundwater and porewater within 10 m of the waterline.

submarine groundwater discharge (SGD) studies found SGD to be significant in this area; thus, it likely plays a major role in ecosystem health (Douglas et al., 2020; Murgulet et al., 2022). For instance, in Nueces Bay, across multiple seasons, SGD was among the highest measured in south Texas, with rates as high as 242 cm·day⁻¹, following a multi-year drought, and as low as 27 cm·day⁻¹, subsequent to extreme flooding (\bar{x} : 99 cm·day⁻¹) (Murgulet et al., 2018).

2.2 Data collection and analyses

2.2.1 Sample collection and sample analyses

A total of 18 Corpus Christi Bay surface water samples were collected within 10 m of the waterline at University Beach beginning on 23 August 2017 and continued until 4 February 2018. Henceforth, we refer to surface water samples from Corpus Christi Bay as surface water samples. All surface water samples

were in line with the groundwater and porewater samples (Figure 1C). Two pre-hurricane surface water samples were collected 2.5 and 1.7 days before the first landfall. Post-hurricane, 11 samples were collected daily beginning on 30 August, the fourth day after the mainland (and second) landfall, and three more samples were collected weekly between 16 September and 30 September. An additional two surface water samples were collected in February 2018. Two porewater samples were collected pre-hurricane landfall and one in February 2018. In addition, six groundwater samples were collected from two nested monitoring wells near the monitoring site (Figure 1C): one developed between 5 and 6 m in the unconfined aquifer (shallow) and another between 10 and 12 m in the semiconfined water producing unit (deep). Groundwater samples were collected from each formation 2 days pre-hurricane, post-hurricane on 20 September, and in February 2018. All samples were analyzed for inorganic nutrients, dissolved organic carbon (DOC), total dissolved

nitrogen (TDN), and DOM molecular characterization. All samples were collected using standard techniques for surface water, porewater, and groundwater (Douglas et al., 2021a).

2.2.2 Inorganic and organic nutrient measurements

Nitrate (NO_3^-), nitrite (NO_2^-), and ammonium (NH_4^+) were measured on a Seal QuAAtro nutrients autoanalyzer (EPA, 2011) at the Geochemical and Environmental Research Group (GERG), College of Geosciences at Texas A&M University College Station, with method detection limits (MDLs; in $\mu\text{mol L}^{-1}$) of 0.11, 0.012, and 0.057, respectively. The MDL is defined as Student's *t* for 99% confidence level times the standard deviation of seven replicate measurements of the same low-level sample or spiked sample. Measurements of DOC and TDN were conducted using a Shimadzu TOC-V analyzer with a nitrogen module, with an MDL of approximately $1 \text{ mg}\cdot\text{L}^{-1}$. Dissolved organic nitrogen (DON) was estimated as the difference between TDN and dissolved inorganic nitrogen ($\text{DIN} = \text{NO}_2^- + \text{NO}_3^- + \text{NH}_4^+$).

2.2.3 Ultrahigh-performance liquid chromatography–Orbitrap fusion Tribrid mass spectrometry

Samples for DOM molecular characterization were collected, processed, and analyzed with UPLC-OT-FT MS as described in detail in Douglas et al. (2021a). Additional OT-FT MS methods and specific OT-FT MS instrument settings can be found in the Supplementary Material. Briefly, samples were collected in 1-L polycarbonate amber bottles previously cleaned with Alconox and HCl solution and rinsed with the sample. Immediately after collection, samples were sterile filtered through 0.2- μm polyethersulfone filters conditioned with 5–10 ml of sample to remove particulates and frozen until processed. Prior to extraction, 100 ml of each sample was acidified to pH 2 with HCl to increase extraction efficiency for organic acids and phenols. DOM samples were then prepared for mass spectrometric analysis using 200 mg, 3 ml Bond Elut-PPL solid phase extraction cartridges following the procedure recommended by Dittmar et al. (2008). Preceding elution of DOM, two cartridge volumes of 0.01 M HCl were passed through the cartridge to completely remove salts and then were dried. The samples were eluted with 6 ml of Optima LC/MS-grade methanol. The methanol eluents were dried in a Centrivap benchtop concentrator and reconstituted with 1 ml of 95:5 water to acetonitrile.

Aliquots of the sample were analyzed on a 1.7- μm ACQUITY UPLC BEH C18 reversed-phase column (Waters, 30 Å, 1.7 μm , 2.1 mm \times 100 mm) via a heated electrospray ionization (H-ESI) source to Orbitrap Fusion Tribrid Mass Spectrometer (Thermo Scientific, Waltham, MA, USA) operated under positive mode. The positive mode was used for its preferential ionization of nitrogen-containing organic matter

to facilitate comparison with and discussion of changes in inorganic nitrogen species. Between each sample analysis, an 8-min column re-equilibration was performed. For MS², the isolation window was set at 0.7 *m/z* while performing both collision-induced dissociation (CID) and higher-energy collisional dissociation (HCD) using an ion trap mass spectrometer as the detector.

Compound Discoverer software 3.1 (Thermo Fisher) was used to identify the DOM compounds according to the following conservative criteria: 1) a signal-to-noise ratio of above 3, 2) a minimum of five mass scans per chromatographic peak, 3) a minimum peak intensity of 50,000, and 4) at least one isotope peak detected. All chromatography spectra retention times (RTs) were aligned using an adaptive curve with a maximum shift of 0.2 min and 5-ppm mass tolerance. The ratio of the M+1 to parent peaks was used to confirm the number of carbon atoms, and the M+2 peak ratio was used to confirm the presence of the S atom in the compound. If multiple adducts were detected (Supplementary Material), all adducts of the same compound were grouped together with an RT tolerance of 0.2 min. Based on our observed analysis, there were limited cases where multiple adducts were detected for the same compounds. A total of 1,427 out of 1,822 compounds detected had a single adduct ($[\text{M}+\text{H}]^+$), and the maximum number of adducts detected for a single compound was 6.

A molecular formula calculator (Molecular Formula Calc version 1.0 NHMFL, 1998) was used to determine empirical formula matches with the following parameters: $\text{C}_{4-100}\text{H}_{4-200}\text{O}_{0-50}\text{N}_{0-10}\text{S}_{0-3}\text{P}_{0-3}$. Molecular formulas that are unlikely to occur in nature or are not chemically possible were removed, as described in detail in Abdulla et al. (2013). Internal standards were not used when analyzing these samples; thus, the calculated masses of the assigned formulas are all within 2.0 ppm of the masses detected by OT-FT MS. For a more detailed description of these analyses, the reader is directed to Douglas et al. (2021a).

2.2.4 Statistical data analysis

The data were gap filled and normalized to constant sum in Compound Discoverer and exported for statistical analyses. Compound presence or absence in each sample was determined if it met or did not meet the four criteria listed above. For absent compounds, a gap filling approach that integrated the area where the peak was expected but not detected was performed to prevent skewing toward missing values (i.e., zero values) in the statistical analyses. No bias is introduced by integrating these gap-filled areas, as they usually correspond to spectra noise. Peak magnitude-weighted O/C_w , H/C_w , and N/C_w were calculated, as described in Douglas et al. (2021a), to characterize each sample and facilitate discussion of DOM composition (Sleighter et al., 2010; Schmidt et al., 2017).

A molecular lability boundary (MLB), developed from FTICR-MS molecular data visualized in van Krevelen diagrams with

chemical class regions, separates the data into more and less labile constituents. This is based on the higher degrees of hydrogen saturation of the protein-, amino sugar-, and lipid-like region linkage to more bioavailable fractions of carbon (D'Andrilli et al., 2015). Constituents of DOM above the MLB at $H/C \geq 1.5$ correspond to more labile material, whereas constituents of DOM below the MLB ($H/C < 1.5$) exhibit less labile, more refractory character (grouping in more lignin-, tannin-, and condensed aromatic-like regions of the van Krevelen diagram). The percentage of more labile constituents (MLB_L) was determined by the number of molecular formulas with $H/C \geq 1.5$ over all O/C (0.0–1.2) divided by the total number of molecular formulas in the sample or by the number of formulas in a heteroatom group, multiplied by 100. Classification of less labile, or more refractory components (MLB_R), from each carbon source was calculated similarly for molecular formulas below the MLB ($H/C < 1.5$). These calculations are defined as chemical species richness for labile and refractory contributions. The diversity of chemical species was calculated by incorporating the normalized peak height of each mass spectral peak to determine the weighted effect of each ionized elemental composition on the overall distribution in each group (i.e., labile: MLB_{wL} or refractory: MLB_{wR}). Although chemical class regions in van Krevelen diagrams contain a degree of ambiguity, and the degree of lability can also be a function of oxygenation; this conservative MLB calculation can provide an unbiased way to distinguish between more or less labile OM by high-resolution MS (D'Andrilli et al., 2015).

Cluster analyses and principal component analyses (PCAs) were performed to assess the temporal variability of DOM composition using SAS 9.4 software. Cluster analyses were performed using PROC CLUSTER with Ward's minimum-variance method after standardizing DOM peak magnitudes with PROC ACELUS, which transforms the data such that the resulting within-cluster covariance matrix is spherical when you suspect the data contain elliptical clusters without known cluster membership or number of clusters, and PROC STANDARD, which creates z-scores for each variable to a mean of 0 and standard deviation of 1. The number of clusters was determined from a visual inspection of the dendrogram and the values of the cubic clustering criteria, pseudo-F, and t^2 statistics. To explore how sample groups differed based on compound class and structure, the O/C and H/C ratios of the assigned molecular formulas for compounds present in each cluster were plotted in van Krevelen diagrams with generalized compound class regions identified (Koch and Dittmar, 2006). The differences in DOM composition between the clusters aid in identifying the potential sources and transformations of compounds in the time series as well as potential environmental drivers.

PCA and van Krevelen diagrams were used to visualize the correlation between multivariate data in the samples. For PCA, the data were standardized to a normal distribution using PROC STANDARD so that scales were the same for all variables. PCA

was performed using the PROC FACTOR procedure in principal components mode with VARIMAX rotation for axis rotation (Douglas et al., 2021a). A sample score plot and a variable loading plot, which shows the distribution of the samples and variables (i.e., individual compounds), respectively, were generated.

Spearman's rho coefficient (r) was used for correlation analyses of nutrients and hydrologic parameters (i.e., water level and creek discharge). This type of analysis is best suited for parameters not normally distributed and are not expected to have a linear relationship, thus making Pearson's correlation coefficient unreliable (Hauke and Kossowski, 2011). For this study, the 95% confidence interval (or p-values ≤ 0.05) is deemed as an indication of a significant correlation.

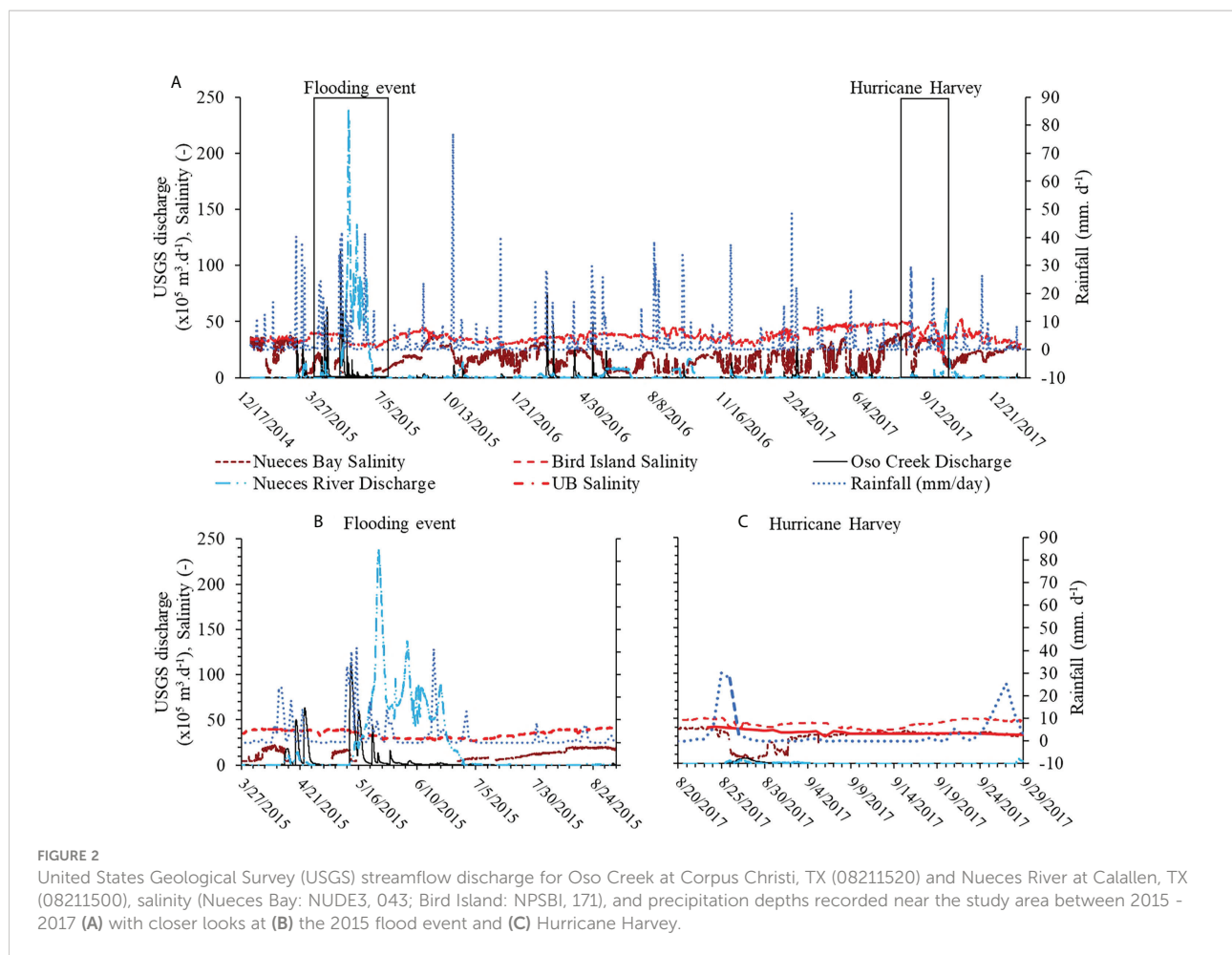
3 Results

3.1 Hydrologic conditions

Hurricane Harvey originated in the Atlantic and rapidly intensified as it approached the Texas coast, reaching a sustained windspeed of 115 knots ($213 \text{ km}\cdot\text{h}^{-1}$)—category 4 status on the Saffir–Simpson scale—before making landfall (NOAA, 2017). It first made landfall on 26 August at 03:00 UTC (25 August at 22:00 local time) approximately 50 km north of Corpus Christi on the northern end of San Jose Island. The second landfall on the Texas mainland occurred approximately 3 h later with sustained windspeeds of 105 knots ($195 \text{ km}\cdot\text{h}^{-1}$) (NOAA, 2017). After stalling over the south and southeast Texas, the storm drifted offshore 3 days later before making another final landfall in southwestern Louisiana on 30 August (Figure 1A).

Hurricane Harvey delivered considerable amounts of precipitation at ~ 125 billion m^3 of rain over the United States (Fritz and Samenow, 2017). Most of the rain received in Texas, up to 152 cm (Blake and Zelinsky, 2018), occurred to the north and northeast of the study area (Figure 1A) with only up to 16 cm measured at the TAMU-CC weather station. Consequently, surface runoff from stream flow discharge (i.e., from Oso Creek or Nueces River) and overland flow were relatively low near the monitoring location (Figures 2A, B).

Oso Creek, which is the nearest source of returned flows to the monitoring area, peaked slightly between the two landfalls but quickly decreased to almost negligible flows (Figures 2C, 3A). Contrary to typical storm impacts, which bring high storm surges and rain that causes flooding, the coastal area southwest of the hurricane's track experienced maximum storm surges of <1 m (Blake and Zelinsky, 2018) with the occurrence of negative storm surge due to the offshore direction of winds (because of the anticlockwise rotation of the storm and the location and orientation of Corpus Christi Bay relative to the storm center). The most significant changes in the area were related to changes in sea level. Water levels within the Nueces Estuary, including Corpus



Christi Bay, fluctuated significantly during and after hurricane landfall, falling approximately 0.1 m below the mean lower low water level (MLLW) during landfall, hovering around the MLLW for approximately 4 days, and falling again to 0.2 m below the MLLW on 1 September (Figure 3A). The water level eventually recovered to mean sea level (MSL) but dropped again (not as severely) before recovering. It is important to note that the largest difference in water level recorded following the first and second landfalls was approximately 0.6 m (Figure 3A) and was captured in the daily sampling. The drop in water level was considerable given that the average depth of Corpus Christi Bay is 3.6 m and the microtidal nature of the estuaries in the northwestern Gulf of Mexico (Gardner et al., 2006).

3.2 Nutrient concentrations

3.2.1 Surface water

Concentrations of NO_3^- , NO_2^- , and NH_4^+ were substantially greater following landfall and the accompanying ~0.5 m drop in water levels from before the storm (Figure 3B). However, only

surface water NH_4^+ had a strong negative correlation with water level (p -value = 0.03), while NH_4^+ and NO_2^- were positively correlated (p -value = 0.02 and p -value < 0.01, respectively) and DOC was negatively correlated (p -value = 0.04) with Oso Creek discharge (Table 1). In contrast, surface water DON concentrations were slightly higher before the hurricane landfall and initially decreased post-landfall (Figure 3C). Concentrations of DON, NO_3^- , NO_2^- , and NH_4^+ fluctuated with a decreasing trend corresponding with the most negative surge, with water levels decreasing to MLLW or lower multiple times over the 4 days after the second landfall. The most negative surge followed 2 days after Harvey's final landfall, though it occurred approximately 280 miles (451 km) northeast of Corpus Christi in southwestern Louisiana. Though concentrations of DON and NH_4^+ initially followed the same trend, they began to fluctuate with inverse trends to each other starting on day 9 while returning to MSL (Figures 3B, C). As DON spiked with a slight drop in salinity in the early days post-landfall, NH_4^+ decreased (Figures 3A, C). Concentrations of NO_3^- remained relatively low but peaked along with DON slightly on day 9 and substantially on day 13 and were overall positively correlated to

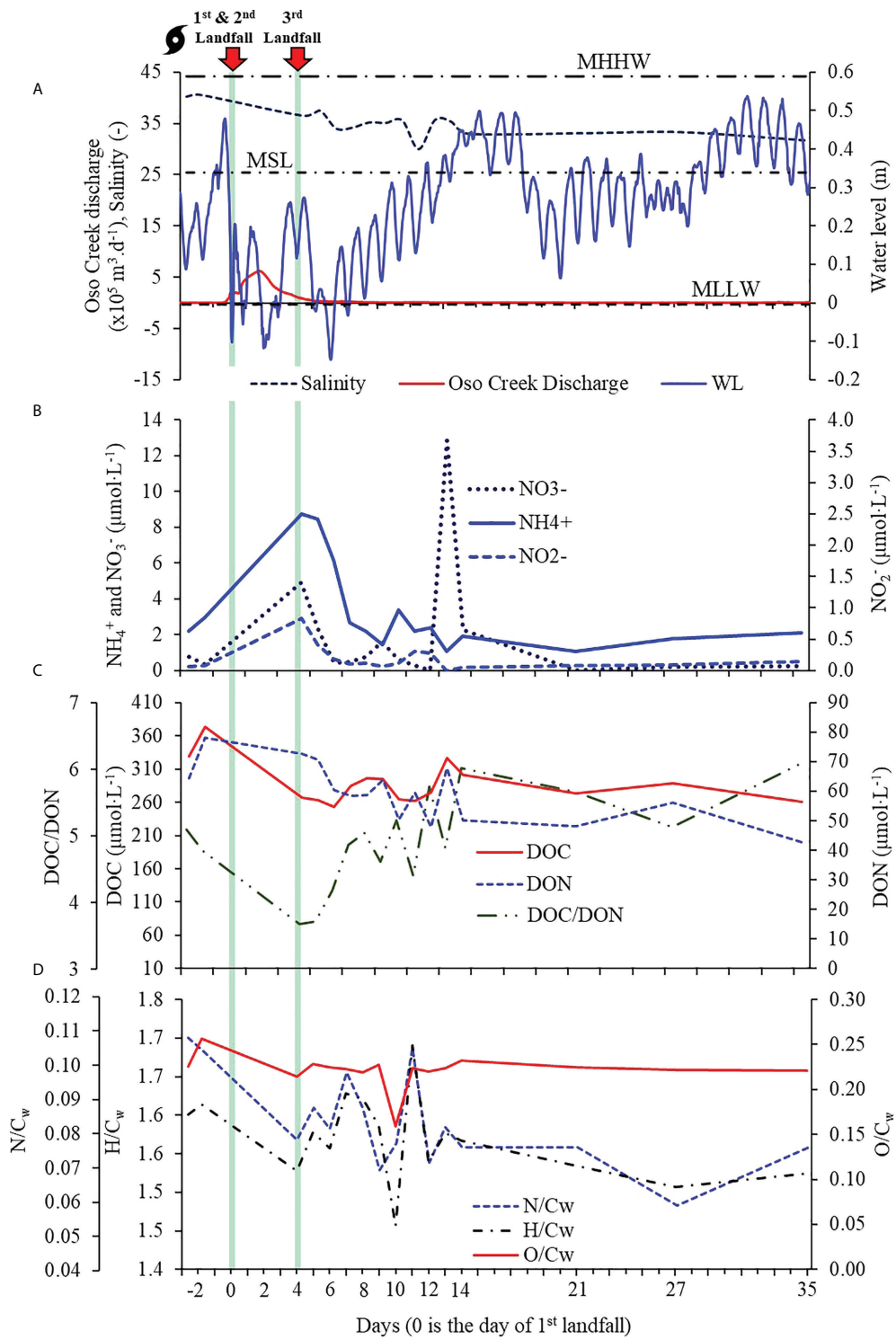


FIGURE 3
 Temporal variation of Corpus Christi Bay surface water. (A) Continuous water level, salinity, and Oso Creek discharge with mean higher high-water level (MHHW), mean sea level (MSL), and mean lower low water level (MLLW) shown. (B) Ammonium, nitrate, and nitrite. (C) Dissolved organic carbon (DOC), dissolved organic nitrogen (DON), and C/N ratios. (D) H/C_w , O/C_w , and N/C_w ratios. Hurricane landfalls are indicated by vertical green bars.

TABLE 1 Spearman's rank correlations for inorganic and organic nutrients, dissolved organic matter chemical composition, and hydrologic metrics.

(n = 18)		Water level	Oso Creek discharge	Salinity	pH
Oso Creek discharge	r	-0.443	1		
	p	0.066			
Salinity	r	-0.203	-0.015	1	
	p	0.418	0.951		
pH	r	0.424	0.157	-0.187	1
	p	0.079	0.534	0.458	
NO ₃ ⁻	r	-0.224	0.210	0.423	0.113
	p	0.371	0.403	0.080	0.656
NO ₂ ⁻	r	-0.329	0.662	-0.189	-0.178
	p	0.182	0.003*	0.453	0.481
NH ₄ ⁺	r	-0.511	0.564	0.451	-0.178
	p	0.030*	0.015*	0.060	0.481
DOC	r	0.199	-0.484	0.583	-0.074
	p	0.428	0.042*	0.011*	0.769
DON	r	-0.337	0.143	0.738	-0.073
	p	0.171	0.570	0.001*	0.773
C:N	r	0.447	-0.467	-0.536	-0.057
	p	0.063	0.050*	0.022*	0.823
Total compounds	r	-0.113	-0.467	0.214	-0.441
	p	0.656	0.051	0.394	0.067
Avg. MW	r	0.424	-0.278	-0.139	-0.062
	p	0.079	0.265	0.581	0.807
O/C _w	r	-0.022	-0.325	0.022	-0.022
	p	0.932	0.188	0.932	0.932
H/C _w	r	-0.470	0.131	0.053	-0.187
	p	0.049*	0.604	0.836	0.458
N/C _w	r	-0.527	0.092	0.071	-0.316
	p	0.025*	0.717	0.779	0.202
S/C _w	r	0.331	-0.356	-0.131	-0.146
	p	0.179	0.147	0.604	0.564
MLB _L	r	-0.240	-0.051	0.044	-0.480
	p	0.337	0.842	0.861	0.044*

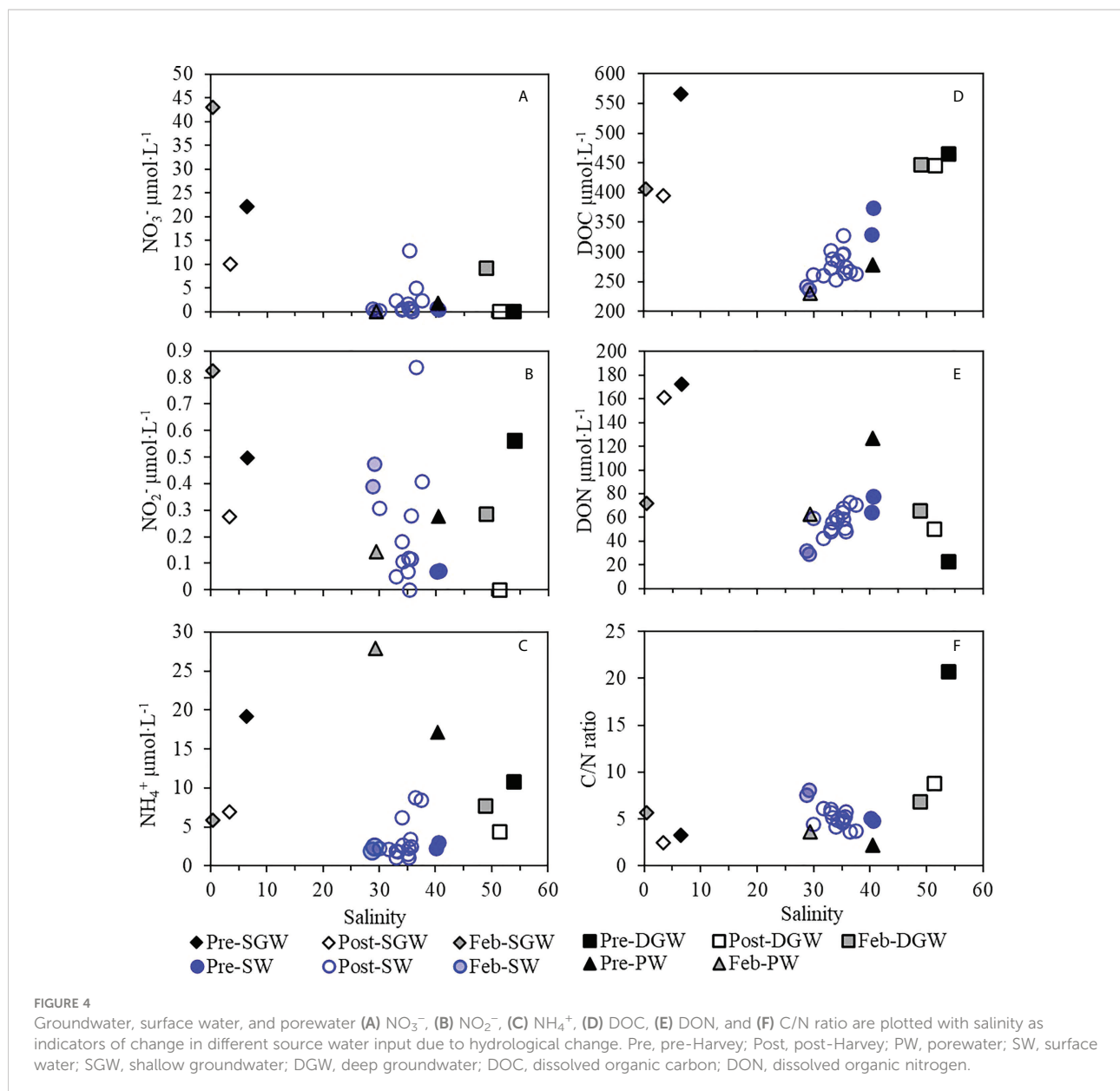
Significant correlations (p-value < 0.05) are shown in bold with an asterisk (*) and weak correlations (p-value < 0.1) are shown in bold italics. DOC, dissolved organic carbon; DON, dissolved organic nitrogen.

each other (p-value < 0.01). Concentrations of NH₄⁺ peaked slightly on day 10 with NO₂⁻ concentrations peaking over the following 2 days before the substantial NO₃⁻ peak on day 13, indicating a recent local pulse of reduced inorganic N followed by nitrification processes.

All nutrients and DOM concentrations stabilized on the lower end for the following 3 weeks, with some slight differences. With a steady overall increasing trend in water levels following day 5, DON and NH₄⁺ seem to have been modulated to a certain extent by salinity fluctuations (p-value < 0.01) and the daily tidal cycle (p-value = 0.03), respectively. Concentrations of DOC were overall lower post-landfalls. Two periods of decreasing concentrations correspond to declines in salinity, which may be pulses of freshwater inflows.

3.2.2 Porewater and groundwater

The groundwater and porewater signatures of different dissolved inorganic and organic nutrients were used in this study, representative of pre- and post-landfall conditions, as means to evaluate the potential for groundwater-surface water interaction. Groundwater in the nearby island water table (e.g., unconfined aquifer) was characterized by low to brackish salinity (0.37–6.47, \bar{x} = 3.1), both pre- and post-landfall, while for the semiconfined (deeper) aquifer, salinities were generally hypersaline (30–54, \bar{x} = 44.3) though slightly fresher post-landfall (Figures 1C, 4). Overall, the salinity of shallow groundwater was lower than that of porewater, surface water, and deep groundwater, likely due to recharge from local rainfall, irrigation, and limited connection with the estuary. Similarly, the



signatures of different dissolved inorganic and organic nutrients reveal shallow groundwater as chemically distinct from deeper groundwater (Figure 4).

While pre- and post-landfall changes in pore- and surface water salinity had trends like the deep and shallow groundwater (e.g., a shift toward lower salinity following the landfall), changes in NO_3^- , NO_2^- , and NH_4^+ concentrations were not consistent (Figures 4A–C). The concentrations of NO_2^- and NO_3^- were the highest in shallow groundwater a few months after the landfall, when the system was more hydrologically stable. Deeper groundwater had a range of NO_2^- concentrations that encompass porewater and most of the surface waters (Figure 4B). Concentrations of NH_4^+ were the highest in porewater a few months post-landfall and about threefold

lower pre-landfall, with levels approaching pre-landfall shallow groundwater (Figure 4C). However, NH_4^+ in porewater exceeded deeper groundwater and post-landfall shallow groundwater. A trend with salinity for groundwater was not obvious for inorganic N, except for NO_3^- , which was the highest at the low salinity end, in shallow groundwater (Figure 4A).

Salinity and DON (Figure 4E) exhibit a negative trend with surface water and porewater falling between the shallow and deeper groundwater fields. However, salinity and DOC (Figure 4D) showed a positive trend in each source, with the pre-landfall samples at the high end and samples from months after landfall at the low end, which may be due to a seasonal effect, but the sample size is too small to speculate further. The largest DON concentrations were in the shallow groundwater

and the lowest in the pre-landfall deeper groundwater. Deeper groundwater DON was higher post-landfall, while the opposite was observed for the shallow aquifer. In comparison, pre-landfall porewaters were more enriched in DON than surface water and deeper groundwater. These trends in DON among the different environments and pre- and post-conditions reveal a mixing pattern between the two aquifers and porewater, and likely exchange with surface water.

3.3 Dissolved organic matter molecular characterization

3.3.1 Overall surface and groundwater dissolved organic matter composition

A total of 1,821 unique compounds were identified by DOM molecular analyses on pre- and post-hurricane surface water and groundwater samples ($n = 26$). Of the total unique compounds, 1,452 (80%) were assigned formulas that were primarily CHO (37.9%), CHON (39.6%), CHONS (11.1%), and CHOS (4.9%), with the remaining as P-containing heteroatoms (CHONP and CHOSP, 3.0%) and CHOP (3.4%). The much lower occurrence of P-containing compounds was expected with ESI+ mode due to the preferential ionization of N-containing compounds (Ohno et al., 2016; Lu and Liu, 2019). An average of 190 formulas were identified in each sample, with the greatest number in the deep ($\bar{x} = 365$ formulas) and shallow groundwater ($\bar{x} = 337$ formulas, Table S2).

The relative abundance of different compounds in surface water was compared during the pre- and post-landfall and the recovery period of 5 months (i.e., February 2018, Figure 5, Table S3). Pre-landfall surface water was dominated by CHON and CHO compounds. Combined N-containing compounds accounted for ~72% of the compounds detected in surface water prior to landfall. Comparatively, on average, the post-landfall relative abundance of CHO increased by 10%, while that

of CHON decreased by ~12%. Also, the average relative abundance of S-containing compounds nearly doubled (10.5%) from pre-landfall (6.6%), with most compounds occurring as NS heteroatoms. After 5 months, the composition of DOM compounds had largely returned to pre-landfall conditions with N-containing compounds once again comprising >70% of the compounds detected, mostly as CHON, and CHO making up most of the rest. However, the relative abundance of S-containing compounds (10.6%) remained like in the post-Harvey samples.

The weighted average molecular element ratios of oxygen to carbon (O/C_w), hydrogen to carbon (H/C_w), and nitrogen to carbon (N/C_w) provide additional insight into DOM composition changes after the landfall. The most oxygenated DOM (i.e., greatest O/C_w) occurred in one February 2018 sample (0.299) and one pre-landfall sample (0.256), while the least oxygenated DOM (i.e., lowest O/C_w , 0.159) occurred on day 10 (Figure 3D; Table S2). All other surface water samples had relatively consistent O/C_w values (0.214–0.232). These O/C_w values were greater than those previously observed in nearby Nueces Bay during a major flood event ($\bar{x} = 0.185$), flood recession ($\bar{x} = 0.176$), and more typical low-flow conditions ($\bar{x} = 0.182$ and 0.178) (Douglas et al., 2021a). This study had similar surface water unweighted O/C elemental ratios (0.22–0.26) as those observed across four rivers located to the northeast of this study's location (0.21–0.27), before (at baseflow) and following Hurricane Harvey (at high flow conditions) (Lu and Liu, 2019). The February 2018 peak and day 10 drop in O/C_w coincided with the lowest H/C_w values observed (1.41 and 1.46, respectively). The highest surface water H/C_w values (i.e., the most saturated DOM samples) were observed pre-landfall (>1.60), on days 7, 8, and 11 (1.62–1.69, cluster 2 in post-landfall samples below), and in the other February 2018 sample (1.78). These values are within the upper range of H/C_w values previously observed in the Nueces Bay study at flood peak (1.44–1.77, $\bar{x} = 1.66$) and flood recession (1.44–1.84, $\bar{x} = 1.67$) (Douglas

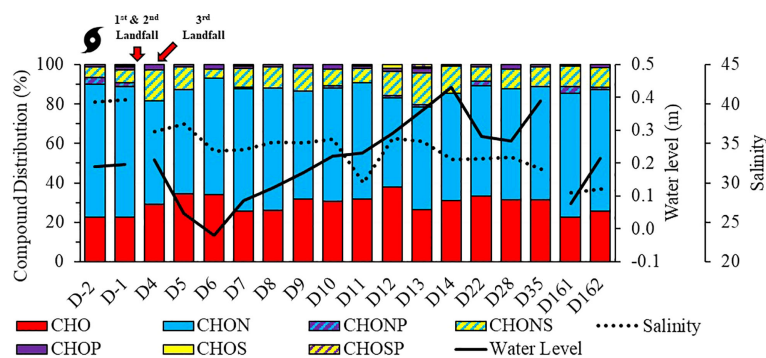


FIGURE 5

Pre-landfall (e.g., D-2 and D-1) and post-landfall (e.g., D4–D35, D161, and D162) surface water DOM molecular composition and percent presence with assigned formulas in relation to bay water level and salinity. DOM, dissolved organic matter.

et al., 2021a) and have similar unweighted elemental H/C ratios (1.48–1.75) to those observed in the monitored rivers at baseflow and high flow conditions (1.46–1.60) (Lu and Liu, 2019). All other post-landfall samples had H/C_w values like the H/C_w values in Nueces Bay during low-flow conditions (\bar{x} = 1.54 and 1.55). The surface water N/C_w followed similar trends to the H/C_w throughout the study period.

For the groundwater DOM samples, 757 unique compounds were detected in the deeper formation (n = 3), 1,012 compounds in the shallow groundwater (n = 3), and 198 compounds in porewater (n = 2); of these, 611 (81%), 803 (79%), and 153 (77%), respectively, were assigned formulas. Surface water had greater relative abundances of CHON than groundwater samples, while groundwater samples had more CHO, CHOS, and CHOP (Figure 6). Surface water and porewater had similar overall DOM compositions. In contrast, shallow groundwater and deeper groundwater were, on average, composed of a greater proportion of CHO (38%–39%) and S-containing compounds (15%–19%) and had the least N-containing compounds (<50%). Shallow groundwater DOM was generally less oxygenated (O/C_w \bar{x} = 0.20) and less saturated (H/C_w \bar{x} = 1.60) than porewater (O/C_w \bar{x} = 0.23, H/C_w \bar{x} = 1.67) and DGW DOM (O/C_w \bar{x} = 0.27, H/C_w \bar{x} = 1.70, Table S2). All groundwater endmembers had generally more saturated DOM than surface water samples, while porewater DOM had similar oxygenation to surface water DOM. Deeper groundwater had the highest percentage of labile compounds (MLB_L \bar{x} = 82.3%), followed by porewater (MLB_L \bar{x} = 79.9%) and shallow groundwater (MLB_L \bar{x} = 70.9%, Table S3). Groundwater had generally higher percentages of labile compounds than surface water (MLB_L \bar{x} = 56.9%).

Cluster analysis and PCA of all surface water and groundwater samples revealed three principal components accounting for ~50% of the variance and comprise 4 clusters

that can be explained by differences in groundwater composition (PC1 and PC3) and the DOM composition post-Harvey (PC2, Figures 7A, B). Principal component 1 accounts for 24.7% of the variance and is driven by the deep groundwater DOM composition (i.e., positive PC1 scores, cluster 1 in Figure 7A). The scores of PC1 were positively correlated with DOC (p-value < 0.01) and negatively correlated with N/C_w (p-value < 0.001), indicating that deep groundwater had higher concentrations of N-depleted OM. Principal component 2 accounts for 13.4% of the total variance and is driven by the difference in DOM composition immediately following Hurricane Harvey (positive PC2 scores, cluster 2) from pre-landfall and February 2018 surface water, shallow groundwater, and porewater composition (negative PC2 scores, cluster 3, Figures 7A, B). On the whole, post-landfall surface water samples contained less CHON and more CHO than porewater and pre-landfall and February 2018 surface water samples (Figures 5, 6). The scores of PC2 positively correlated with pH and S/C_w (p-values < 0.01) and negatively correlated with H/C_w, N/C_w, and NH₄⁺ (p-values < 0.05), indicating that post-landfall DOM was less saturated and processed than other samples. The only factor to have a positive relationship with water level (p-value = 0.05) and a weak positive relationship with Oso Creek discharge (p-value = 0.07) was PC2. The difference in shallow groundwater DOM composition was revealed in PC3, which accounts for 12.4% of the variance and is mainly driven by the unique DOM composition of pre-landfall shallow groundwater (cluster 4, positive PC3 scores, Figure 7B) that had less N (%CHON 30.6, N/C_w 0.06) and a lower percentage of labile compounds (MLB_L 66.3) compared to the other groundwater samples. Principal component 3 was positively correlated with NO₃⁻ (p-value < 0.01), weakly correlated with DOC (p-value = 0.06), and negatively correlated with O/C_w and N/C_w (p-values < 0.05).

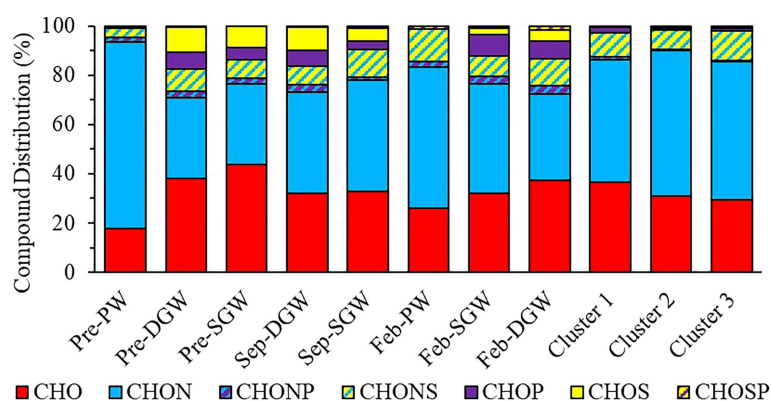


FIGURE 6

DOM molecular composition and percent presence with assigned formulas for pre- and post-landfall (September and February), porewater (PW), and shallow (SGW) and deeper (DGW) groundwater. DOM, dissolved organic matter.

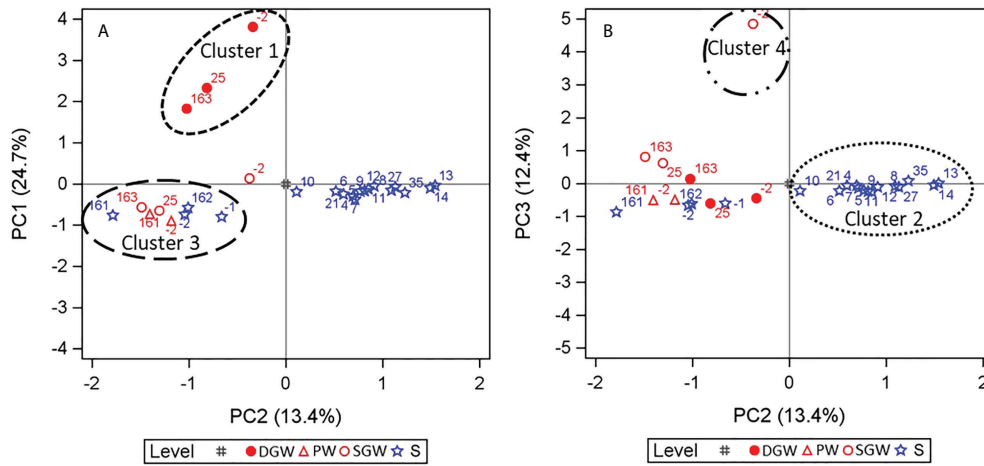


FIGURE 7
Principal components analysis for (A) PC 1 vs PC 2 and (B) PC 3 vs PC 2 comparisons for all surface water (S), shallow groundwater (SGW), deeper groundwater (DGW), and porewater (PW) samples. Cluster analysis results are indicated.

3.3.2 Post-Harvey dissolved organic matter composition

Cluster analysis and PCA of only post-landfall daily molecular data revealed two principal components and three

different groups: cluster 1 (days 4, 5, 6, 9, 10, 12, 22, and 28), cluster 2 (days 7, 8, and 11), and cluster 3 (days 13, 14, and 35) (Figure 8). Explaining ~20% of the variance in the post-landfall DOM composition, PC1 is driven by the difference

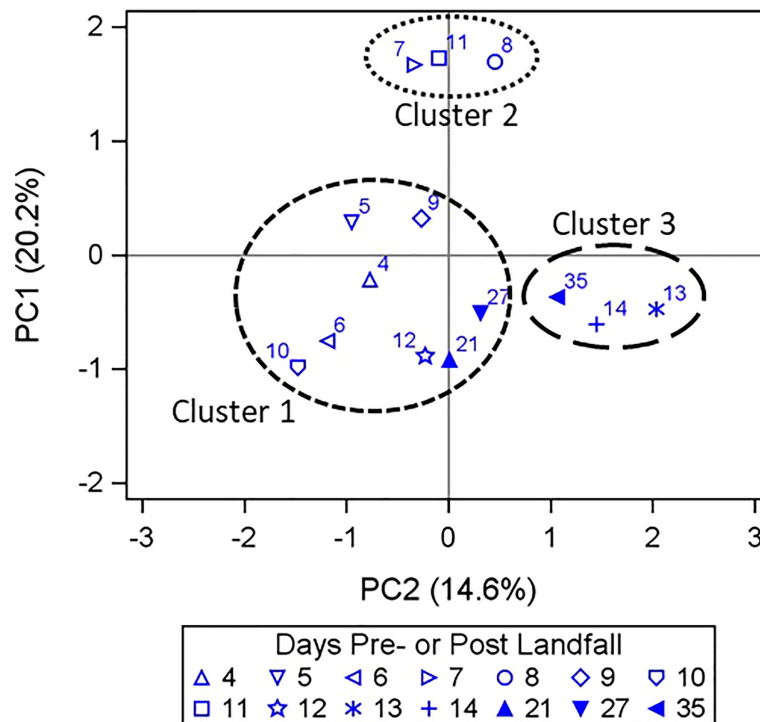


FIGURE 8
Principal components analysis for post-landfall surface water. Cluster analysis results are shown and include surface water samples labeled by days since the initial landfall. The * symbol is defined in the legend with all other symbols. * is station 13.

of days 7, 8, and 11 (positive PC1 scores, cluster 2) from the other post-landfall samples. Cluster 2 had 266 (77%) assigned compounds with a higher presence of CHON and lower CHO than cluster 1 (Figure 9A). Samples in PC1/cluster 2 (Figure 9B) were positively correlated with H/C_w (p-value < 0.01) and N/C_w (p-value = 0.04) and weakly positively correlated with Oso Creek discharge (p-value = 0.06). In general, cluster 2 had more saturated DOM (H/C_w \bar{x} = 1.65) with a greater labile nature (MLB_L \bar{x} = 55.9%, MLB_{wL} \bar{x} = 75.4%) than either cluster 1 (H/C_w \bar{x} = 1.54, MLB_L \bar{x} = 53.7%, MLB_{wL} \bar{x} = 58.8%) or cluster 3 (H/C_w \bar{x} = 1.56, MLB_L \bar{x} = 55.2%, MLB_{wL} \bar{x} = 61.2%).

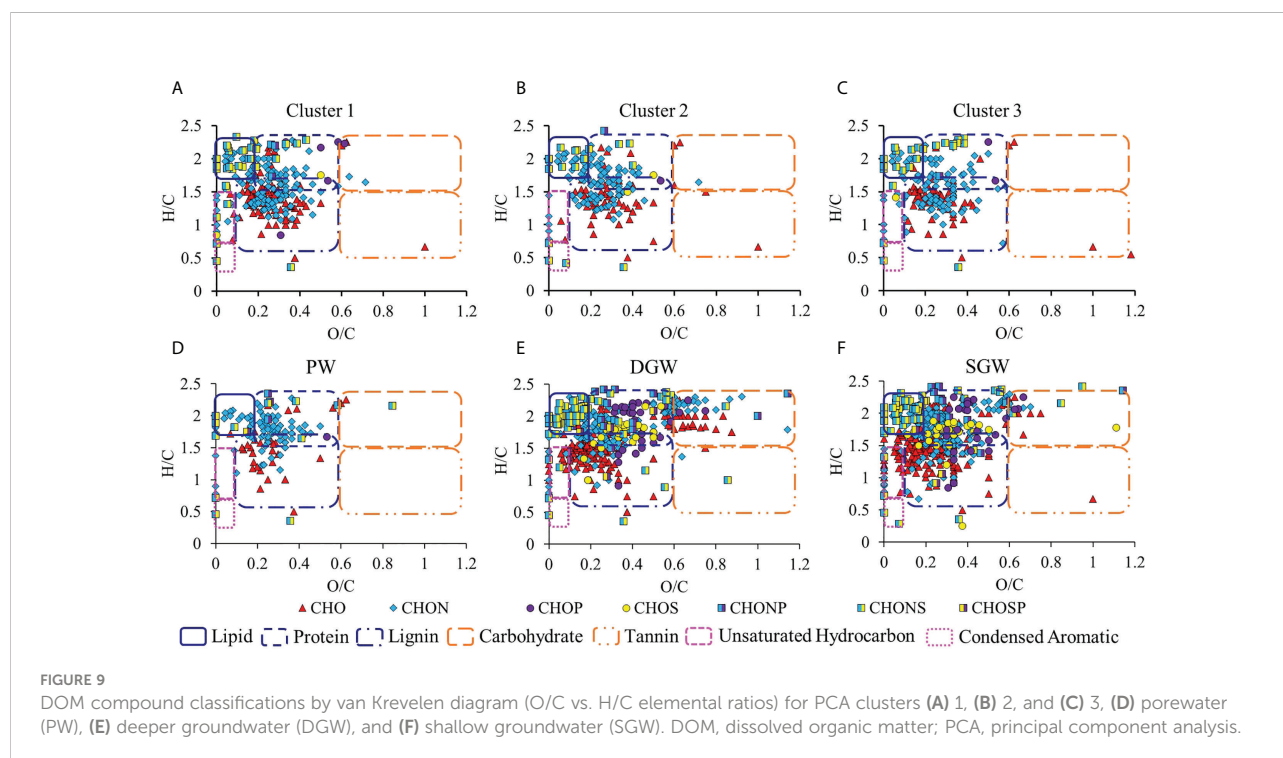
An additional ~15% of the DOM variance is explained by PC2 and is driven by the difference between the more immediate post-landfall samples (negative PC2 scores) and the later post-landfall samples (positive PC2 scores), which loosely match cluster 1 and cluster 3, respectively. The PC2 scores were positively correlated with DOC (p-value = 0.03) and water level (p-value < 0.01) and negatively correlated with NO₂⁻ (p-value = 0.05), NH₄⁺ (p-value < 0.01), and Oso Creek discharge (p-value = 0.05). Cluster 1 samples had 313 assigned formulas comprised of mainly CHON, CHO, and CHONS (Figure 9A).

Cluster 3, with 270 (72%) assigned compounds, had a similar presence of CHON and CHO as cluster 2, but with a higher percentage of CHONS than clusters 1 and 2 (Figures 6, 9). As mentioned above, samples part of cluster 3 had less saturated DOM with a less labile nature than cluster 2 while slightly more

saturated DOM with a more labile nature than cluster 1. The grouping of DOM constituents on the van Krevelen diagram regions shows similarities among the other two clusters, a mix of marine and terrestrial influences (Figure 9).

4 Discussion

Hurricane Harvey is a relevant example of how a warming climate may affect storm evolution and impact different coastal areas. For instance, Hurricane Harvey's path was unusual, reversing its course, making landfall twice, and producing record rainfall in less than a week with major flooding for the Houston/Galveston coastal region and other low-lying areas to the south (Yan et al., 2020). Although stream flow discharge and freshwater inflow to estuaries were significant to the east of the hurricane center (e.g., Galveston Bay was converted into a freshwater system) (Steichen et al., 2020), there were negligible impacts from flooding to the west, and freshwater inflows to Corpus Christi Bay were relatively low when compared to those of other wet events (Figure 2). However, as previously mentioned, the impact of Hurricane Harvey in the Nueces Estuary was mostly felt through negative surges caused by the southerly direction of winds and very limited freshwater inflows. These negative surges were found to act as short-term pulses of inorganic nutrients and DOM with slightly more refractory molecular characteristics.



4.1 Hydrologic changes and relationships to nutrient supply

Given that Oso Creek feeds into Oso Bay, which discharges approximately 1.5 km from the monitoring site (Figure 1B), one might expect it to reflect in the chemistry of Corpus Christi Bay. Following Hurricane Harvey, a peak in stream discharge followed the slight increase in precipitation (23 cm), but in magnitudes similar to or smaller than those of other non-tropical cyclone precipitation events throughout the year (Figure 2). Thus, a significant influence from this nearby creek was not expected to directly affect the water chemistry through surface discharges. However, precipitation within the watersheds feeds into the bay through increases in upstream creek levels that serve as short-term aquifer recharge periods (Charette et al., 2008). Felix and Murgulet (2020) determined that Hurricane Harvey rain near the monitoring site had NO_3^- of 10.4 μM and NH_4^+ of 5.7 μM . Since most of the incident rain occurred within the first few days of landfall, wet deposition of inorganic N may also be a source, both directly and indirectly through aquifer recharge and subsurface runoff. Compounded by a sudden drop in sea level, increased groundwater levels due to recharge lead to steepening hydraulic gradients toward the coast that act as short-term hydrologic pulls and input of groundwater further offshore from the shoreline.

Previous studies within the Nueces Estuary have found SGD contributions to be significant (Douglas et al., 2020; Murgulet et al., 2022), with important fluxes of nutrients and DOM that could impact ecosystem health (Douglas et al., 2021a; Douglas et al., 2021b). Though groundwater is generally rich in NO_3^- (Kennedy et al., 2009; Duffner et al., 2021), transport from aquifers to estuaries facilitates conversion to, and accumulation of, NH_4^+ in saline and anoxic porewaters (Santos et al., 2009; Lopez et al., 2020; Wong et al., 2020; Douglas et al., 2021b). From the long-term analyses, surface water NH_4^+ is negatively correlated with water level (p-value = 0.03) and positively with creek discharge (p-value = 0.02). In contrast, NO_3^- has no relationship with either water level or creek discharge (p-value = 0.37 and p-value = 0.40, respectively). Furthermore, the occurrence of NO_2^- in the surface water is an indication of a recent pulse of NH_4^+ , which is rapidly nitrified (Moosdorf et al., 2021). Thus, one possible explanation for the input of NH_4^+ , which was overall the dominant form of inorganic N at this nearshore location, particularly around the third landfall (Figures 3A, B), is related to the short-term hydrologic changes that act as flushing events of porewater, with increases due to groundwater inputs of both NO_3^- (shallow oxic groundwater) and NH_4^+ (deeper anoxic groundwater).

Additionally, the occurrence of NO_2^- in porewater and deep groundwater accompanied by low NO_3^- and high DOC and NH_4^+ concentrations indicate that dissimilatory nitrate reduction to ammonium (DNRA) may be occurring. In estuarine sediments, DNRA competes with denitrification and conserves N as NH_4^+

rather than removing it as N_2 through denitrification (Giblin et al., 2013). While DNRA and denitrification have similar requirements (i.e., anoxic conditions, available NO_3^- and organic substrates), DNRA is thought to be favored in systems with high carbon and low NO_3^- content (Burgin and Hamilton, 2007), such as the porewater and deep groundwater in this study. In addition to DNRA, ammonification of organic matter within the sediment (Abdulla et al., 2018) or photooxidation of new organic matter introduced with SGD may also produce NH_4^+ (Hansell and Carlson, 2015). Even though the rates of NH_4^+ production from these processes cannot be well constrained from the current data set, the lack of correlation between NO_2^- (p-value = 0.45), or weak positive relationships between NO_3^- (p-value = 0.08) and NH_4^+ (p-value = 0.06) with salinity, favors processing rather than mixing. Short bursts of remineralized and terrestrially derived inorganic nitrogen, *via* subterranean inputs, such as SGD found to increase following Hurricane Harvey in the adjacent Nueces Bay and Upper Laguna Madre (Murgulet et al., 2022), are a plausible cause for the observed trends. Other recent studies found storm events responsible for higher SGD rates and nutrient fluxes to the coastal ocean, although these occurrences were mostly driven by high precipitation rates and subsequent recharge (McKenzie et al., 2021; Diego-Feliu et al., 2022).

No obvious trend was observed in surface water DOC and DON as dependent on sea level. In contrast, an increase in creek discharge had an inverse relationship with DOC and C/N and no relationship with DON (Table 1). Assuming higher creek water levels could be associated with recharge events to the shallow aquifers, the negative correlation could signify a terrestrial source of organic matter from recent runoff and groundwater discharge to the bay. Furthermore, both DOC and DON concentrations in surface water had positive relationships with salinity (p-values 0.01 and <0.01), suggesting concentrations were mainly driven by the mixing of saline/fresh inputs, which, given this study's hydroclimatic conditions, may be hinting at benthic and deeper groundwater inputs (i.e., porewater flushing events associated with hydrologic pulls). This may be further supported by the observed decrease in the surface water and deeper groundwater C/N post-landfall (Figures 3C, 4F), followed by a progressive increase to values slightly higher than pre-landfall.

4.2 Hydrologic impacts on dissolved organic matter composition

Pre-landfall, N-containing compounds were more abundant when compared to the first days of sampling post-landfall. Following Hurricane Harvey, samples uniquely grouped in cluster 1 displayed a shift toward a DOM pool of lower average O/C_w and H/C_w ratios with greater abundances of CHO compounds in the lignin-like and unsaturated hydrocarbon-like class regions (Figures 6, 9A), more like the

shallow groundwater grouping (Figure 9F). The occurrence of more CHO compounds has been related to an increasingly higher presence of terrigenous DOM (Schmidt et al., 2017). On average, cluster 1 samples also had the least labile characteristics of the post-landfall samples (Table S2) and had more unsaturated CHO and less N-containing compounds (Figure 9A). Since terrestrial DOM is characterized by more aromatic compounds and a greater CHO composition and given the observed correlations described above, as well as the dominance of CHO compounds in the nearby fresh aquifer (Figure 6), a potentially more significant contribution from advective and fresher SGD is hypothesized. Additionally, the grouping of more DOM constituents in the unsaturated hydrocarbon- and lignin-like regions of the van Krevelen diagram for cluster 1 is comparable to that of the shallow groundwater (Figure 9F). The change to lower surface water levels and higher creek discharge seems to have played a role in these observed shifts, which also favored inputs of DOC and NH_4^+ , likely resulting from the enhanced flushing of porewaters caused by hydrologic pulls.

Of the post-landfall, several days exhibited a shift to higher N-like compounds, of higher saturation and less refractory state, and corresponded with overall rising bay water level (e.g., cluster 2) or a return to average mean sea level (e.g., cluster 3). The higher presence of N-containing compounds may be attributed to a more autochthonous source like benthic fluxes of DOM enriched by microbial activity (Schmidt et al., 2009) or a more aliphatic marine-dominant source of DOM. The high H/C_w values in cluster 2 align with those from Nueces Bay during flooding and flood recession (Douglas et al., 2021a) and approach the high porewater ($\bar{x} = 1.67$) and deeper groundwater ($\bar{x} = 1.7$) values. These characteristics may be reflective of greater microbial influence, thus a more autochthonous source affected by seawater recirculation rather than more advective fresh terrestrial inputs. Both deeper groundwater and porewaters are of high salinity and are expected to be more interlinked (Figure 1C) and favor microbial processes to dominate the porewater DOM signature and those of the associated benthic fluxes. However, cluster 3, including days more distant from the landfall (Figures 5, 6), was characteristically like cluster 2 as far as the presence of CHON and CHO compounds, but with a higher percentage of CHONS than clusters 1 and 2 (Figures 6, 7). The DOM pool was less saturated and less labile than cluster 2 while slightly more saturated and more labile than cluster 1, potentially a mix of marine and terrestrial influences as expected during more stable conditions.

Interestingly, although proportionally lower when compared to CHO and CHON, the presence of S-containing compounds increased post-landfall. This increase could be attributed to DOM sulfurization (e.g., reactions of DOM with aqueous sulfide), which was observed to increase with increasing DOM aromatic-, carbonyl-, and carbonyl-C content and facilitates

Hg-sulfate-DOM bioavailability to a methylating bacterium (Graham et al., 2017). Since sulfide may favor nitrate reduction (Li et al., 2022), the presence of S-containing compounds may provide some evidence for the production of NH_4^+ from DNRA as indicated earlier. Sulfide produced from microbial sulfate reduction can be readily incorporated into DOM. Sulfate reduction is the predominant anaerobic microbial process of organic matter mineralization in marine sediments. Recent studies reveal that sulfate reduction occurs in sulfate-rich sediments and even in deeper, methanogenic sediments at very low background concentrations of sulfate (Glombitza et al., 2016). Similar to NH_4^+ , sulfurized DOM generally buried in dissolved form in porewaters (Lau and Del Giorgio, 2020) during lower advective fluxes of SGD would likely diffuse out of sediments, particularly during storm events. For instance, Dixon et al. (2014) identified evidence of benthic resuspension events of degraded, planktonic organic matter in an estuary during high winds and turbulent conditions when porewater flushing is enhanced.

Enhanced flushing of biodegraded organic matter from bottom sediments or deeper anoxic formations may occur during hydrogeologic pulls. Days with larger inputs of S-containing DOM may reflect inputs from the deeper aquifer with characteristically higher salinity and S-like compounds when compared to other types of inputs (Figures 5, 6). Fluctuations in sea level have the ability to influence SGD on both short- and long-term scales, with tidal pumping effects driving short bursts of groundwater into seawater (Kim and Hwang, 2002; Taniguchi and Iwakawa, 2004). Although no continuous groundwater level measurements were recorded for the duration of the study, the detected statistical similarities in the DOM molecular composition between groundwater and surface water post-landfall, the presence of chemically unstable inorganic N (e.g., NO_2^-) species, porewater nitrogen enrichment (e.g., NH_4^+), and disproportionately higher DOC versus DON inputs (e.g., higher DOC/DON ratios) suggest that hydrologic pulls have enhanced the existent nearshore groundwater input.

Episodic surface runoff may be responsible for inputs of N-rich DOM but of lower H/C_w elemental ratios. Lu and Liu (2019) showed a decrease in the H/C_w ratio during the high-flow events (1.52 to 1.51 in ESI+) associated with Hurricane Harvey in the rivers to the northeast and determined that at a high stage the DOM riverine pool was increasingly dominated by terrigenous-like inputs. For this study, however, the H/C_w ratio increases overall following the hurricane landfall up to 12 days, with a decline to 1.4 after 35 days (Figure 3D). The decline is accompanied by a steady decrease in salinity (Figure 3A) and DOC and NO_3^- concentrations, suggesting lagged surface runoff inputs of terrigenous DOM. Generally, terrestrial sources of DOM including livestock wastewater (Sun et al., 2017) and pasture, forest, and urban/suburban runoff (Seitzinger et al., 2002) are $\sim 42\% \pm 25\%$ bioavailable due to their expected high abundance of amino acids, peptides, and urea. Other allochthonous sources

are wastewater discharges, believed to be a source of contamination in flooded areas, with up to 80% bioavailability when the optimum environmental conditions were met (Sun et al., 2017). In addition, DON in the rain that recharges surficial aquifers is reported to be 20% to 75% bioavailable (Seitzinger and Sanders, 1999). Stormwater runoff and tidal changes were found to increase the bioavailability of DOM with predominant inputs of humic-like compounds in the wet season and protein-like components in the dry season (Smith et al., 2021). In this study, the negative surge was linked to an increase in the humic-like compounds, which are predominant in the nearshore groundwater but were also found to increase in Nueces Bay following the 2015 flooding event (Douglas et al., 2021a). Because low-molecular-weight DOM compounds can be sufficiently labile, uptake along the river course (Gardner and Stephens, 1978) may limit their input to coastal waters unless associated with pulse-shunt events of short residence times and inundation (Douglas et al., 2021a). With the limited freshwater inflows to the Nueces Estuary associated with Hurricane Harvey, the increasing presence of CHO compounds in the nearshore environment is more likely reflective of subsurface transport of DOM, given similarities to the nearby groundwater.

5 Conclusion

Recent hurricanes have exerted a climatic fingerprint on the DOM sources to marine environments through increased storm surges and flooding. In the Nueces Estuary, the impact of Hurricane Harvey manifested through negative surges and limited surface runoff. These enhanced tidal pumping mechanisms are caused by sudden drops in sea level and steepening of the hydraulic gradient between the water table and the sea. Collectively, this study suggests that the inorganic and organic nutrient compositions of surface water in the nearshore environment of Corpus Christi Bay changed significantly a few days after the landfall of Hurricane Harvey. This “hydrologic pull”, or enhanced flushing of porewater, led to larger inputs of NH_4^+ following the landfalls with a switch to a large pulse of NO_3^- combined, an increase in salinity approximately 2 weeks post-landfall, and the mean sea level approaching higher high. However, DOC and DON were lower following the landfalls with a return to slightly higher pre-landfall signatures that corresponded with the NO_3^- pulse. However, the DOC input in relation to DON for the recovery period up to 12 days after the first landfall was proportionally higher, with the DOC/DON ratio reaching the highest value at the salinity and NO_3^- peak. Comparatively, a transition from a proportionally higher marine N-dominated DOM pool before the hurricane to a higher terrestrial CHO- and S-like (or sulfurized) DOM composition was observed up to a month after the first landfall. These changes are observed to mimic nearshore groundwater signatures, in which the CHO- and S- are more abundant when compared to surface water. A shift to larger terrestrially derived

DOM sources occurs on most days post-landfall, although streamflow discharge peaked only slightly 2 days after the first mainland landfall. The increased presence of S-like DOM supports the hypothesis that terrigenous DOM is mobilized and exported to the estuary *via* SGD that includes both recirculated seawater through bottom sediments and terrestrial groundwater fluxes. Results of this study, although representative of Corpus Christi Bay nearshore to an island environment, indicate significant changes in forms of DIN and DOM inputs with mobilization of slightly less labile and unsaturated terrestrial sources, linked to nearshore subsurface runoff (e.g., freshwater table aquifer). While this work captured the immediate impact of a hurricane on a nearshore environment, future work is recommended to enhance our understanding pertaining to the effects of negative surges on SGD and the associated nutrient fluxes for an improved understanding of the physicochemical and biological changes following a large storm event within semiarid estuaries.

Data availability statement

The original contributions presented in the study are included in the article/Supplementary Material. Further inquiries can be directed to the corresponding author.

Author contributions

JF and AD contributed to sample collection. AD, DM, MG, and KD performed all formal analyses, created all visuals, and wrote the original manuscript. MG conducted the DOM molecular characterization experiments under the supervision of AD, HA, and DM. JF and HA helped in the expansion of concepts, manuscript preparation, and data synthesis. All authors contributed to the article and approved the submitted version.

Funding

The Center for Water Supply Studies at Texas A & M University-Corpus Christi (TAMU-CC) financially supported this research. Funds for open access publication fees were received from the TAMU-CC library.

Acknowledgments

The DOM UPLC-OT-FT MS analyses were possible with the support from the National Science Foundation under grant number OCE-1626494 to HAA. We would like to thank the McNair Scholars Program and the Center for Water Supply Studies (CWSS) at Texas A&M University-Corpus Christi (TAMU-CC) for providing MG with this opportunity to

complete a research project as an undergraduate research assistant by providing funding, equipment, and additional resources and data used in this project. We would like to thank the graduate students in the CWSS for their help with the sample collection and processing and Ph.D. candidate Kevin Nelson (TAMUCC) for his assistance in retrieving Hurricane Harvey storm track data and his consultations on hurricane dynamics and terminology.

Conflict of interest

The authors declare that the research was conducted in the absence of any commercial or financial relationships that could be construed as a potential conflict of interest.

References

- Abdulla, H. A., Burdige, D. J., and Komada, T. (2018). Accumulation of deaminated peptides in anoxic sediments of Santa Barbara basin. *Geochimica Cosmochimica Acta* 223, 245–258. doi: 10.1016/j.gca.2017.11.021
- Abdulla, H. A., Minor, E. C., Dias, R. F., and Hatcher, P. G. (2013). Transformations of the chemical compositions of high molecular weight DOM along a salinity transect: using two dimensional correlation spectroscopy and principal component analysis approaches. *Geochimica Cosmochimica Acta* 118, 231–246. doi: 10.1016/j.gca.2013.03.036
- Akkanen, J., Vogt, R. D., and Kukkonen, J. V. (2004). Essential characteristics of natural dissolved organic matter affecting the sorption of hydrophobic organic contaminants. *Aquat. Sci.* 66 (2), 171–177. doi: 10.1007/s00027-004-0705-x
- Ashworth, J. B., and Hopkins, J. (1995). *Major and minor aquifers of Texas* (Austin, TX: Texas Water Development Board), 69.
- Baker, E. T. (1979). *Stratigraphic and hydrogeologic framework of part of the coastal plain of Texas*. Austin, TX: Report 236, Texas Department of Water Resources
- Bauer, J., and Bianchi, T. (2011). 5.02–dissolved organic carbon cycling and transformation. *Treatise Estuar. Coast. Sci.* 5, 7–67. doi: 10.1016/B978-0-12-374711-2.00502-7
- Behrens, E. W. (1966). Surface salinities for Baffin bay and Laguna madre, Texas, April 1964–march 1966. *Publications Institute Mar. Science Univ. Texas* 11, 168–179.
- Bianchi, T., and Bauer, J. (2011). 5.03–particulate organic carbon cycling and transformation. *Treatise Estuar. Coast. Sci.* 5, 69–117. doi: 10.1016/B978-0-12-374711-2.00503-9
- Bighash, P., and Murgulet, D. (2015). Application of factor analysis and electrical resistivity to understand groundwater contributions to coastal embayments in semi-arid and hypersaline coastal settings. *Sci. Total Environ.* 532, 688–701. doi: 10.1016/j.scitotenv.2015.06.077
- Blake, E. S., and Zelinsky, D. A. (2018). “Hurricane Harvey,” in *National hurricane center tropical cyclone report. rep. no. AL092017* (Washington, DC: National Oceanic and Atmospheric Administration).
- Boyer, J. N., Dailey, S. K., Gibson, P. J., Rogers, M. T., and Mir-Gonzalez, D. (2006). The role of dissolved organic matter bioavailability in promoting phytoplankton blooms in Florida bay. *Hydrobiologia* 569 (1), 71–85. doi: 10.1007/s10750-006-0123-2
- Burgin, A. J., and Hamilton, S. K. (2007). Have we overemphasized the role of denitrification in aquatic ecosystems? *A Rev. nitrate removal pathways. Front. Ecol. Environ.* 5 (2), 89–96. doi: 10.1890/1540-9295(2007)5[89:HWOTRO]2.0.CO;2
- Carlson, C. A., and Hansell, D. A. (2015). *Biogeochemistry of marine dissolved organic matter* (London: Academic Press), 65–126.
- Charette, M., Moore, W., and Burnett, W. (2008). Uranium-and thorium-series nuclides as tracers of submarine groundwater discharge. *Radioactivity Environ.* 13, 155–191. doi: 10.1016/S1569-4860(07)00005-8
- Chen, S., Lu, Y., Dash, P., Das, P., Li, J., Capps, K., et al. (2019). Hurricane pulses: small watershed exports of dissolved nutrients and organic matter during large storms in the southeastern USA. *Sci. Total Environ.* 689, 232–244. doi: 10.1016/j.scitotenv.2019.06.351
- Chiou, C. T., Malcolm, R. L., Brinton, T. I., and Kile, D. E. (1986). Water solubility enhancement of some organic pollutants and pesticides by dissolved humic and fulvic acids. *Environ. Sci. Technol.* 20 (5), 502–508. doi: 10.1021/es00147a010
- D’Andrilli, J., Cooper, W. T., Foreman, C. M., and Marshall, A. G. (2015). An ultrahigh-resolution mass spectrometry index to estimate natural organic matter lability. *Rapid Commun. mass spectrometry* 29 (24), 2385–2401. doi: 10.1002/rcm.7400
- D’Andrilli, J., Junker, J. R., Smith, H. J., Scholl, E. A., and Foreman, C. M. (2019). DOM composition alters ecosystem function during microbial processing of isolated sources. *Biogeochemistry* 142 (2), 281–298. doi: 10.1007/s10533-018-00534-5
- Denis, M., Jeanneau, L., Petitjean, P., Murzeau, A., Liotaud, M., Yonnet, L., et al. (2017). New molecular evidence for surface and sub-surface soil erosion controls on the composition of stream DOM during storm events. *Biogeosciences* 14 (22), 5039–5051. doi: 10.5194/bg-14-5039-2017
- DeVilbiss, S. E., Zhou, Z., Klump, J. V., and Guo, L. (2016). Spatiotemporal variations in the abundance and composition of bulk and chromophoric dissolved organic matter in seasonally hypoxia-influenced green bay, lake Michigan, USA. *Sci. Total Environ.* 565, 742–757. doi: 10.1016/j.scitotenv.2016.05.015
- Diego-Feliu, M., Rodellas, V., Alorda-Kleinglass, A., Saaltink, M., Folch, A., and Garcia-Orellana, J. (2022). Extreme precipitation events induce high fluxes of groundwater and associated nutrients to the coastal ocean. *Hydrology Earth System Sci.*, 1–27. doi: 10.5194/hess-2021-594
- Dittmar, T., Koch, B., Hertkorn, N., and Kattner, G. (2008). A simple and efficient method for the solid-phase extraction of dissolved organic matter (SPE-DOM) from seawater. *Limnology Oceanography-Methods* 6, 230–235. doi: 10.4319/lom.2008.6.230
- Dixon, J. L., Osburn, C. L., Paerl, H. W., and Peierls, B. L. (2014). Seasonal changes in estuarine dissolved organic matter due to variable flushing time and wind-driven mixing events. *Estuarine Coast. Shelf Sci.* 151, 210–220. doi: 10.1016/j.ecss.2014.10.013
- Douglas, A. R., Murgulet, D., and Abdulla, H. A. (2021a). Impacts of hydroclimatic variability on surface water and porewater dissolved organic matter in a semi-arid estuary. *Mar. Chem.* 235, 104006. doi: 10.1016/j.marchem.2021.104006
- Douglas, A. R., Murgulet, D., and Montagna, P. A. (2021b). Hydroclimatic variability drives submarine groundwater discharge and nutrient fluxes in an anthropogenically disturbed, semi-arid estuary. *Sci. Total Environ.* 755, 142574. doi: 10.1016/j.scitotenv.2020.142574
- Douglas, A. R., Murgulet, D., and Peterson, R. N. (2020). Submarine groundwater discharge in an anthropogenically disturbed, semi-arid estuary. *J. Hydrology* 580, 124369. doi: 10.1016/j.jhydrol.2019.124369

Publisher’s note

All claims expressed in this article are solely those of the authors and do not necessarily represent those of their affiliated organizations, or those of the publisher, the editors and the reviewers. Any product that may be evaluated in this article, or claim that may be made by its manufacturer, is not guaranteed or endorsed by the publisher.

Supplementary material

The Supplementary Material for this article can be found online at: <https://www.frontiersin.org/articles/10.3389/fmars.2022.961206/full#supplementary-material>

- Duan, S., Bianchi, T. S., Shiller, A. M., Dria, K., Hatcher, P. G., and Carman, K. R. (2007). Variability in the bulk composition and abundance of dissolved organic matter in the lower Mississippi and pearl rivers. *J. Geophysical Research: Biogeosciences* 112 (G2), 12. doi: 10.1029/2006JG002006
- Duffner, C., Wunderlich, A., Schloter, M., Schulz, S., and Einsiedl, F. (2021). Strategies to overcome intermediate accumulation during *in situ* nitrate remediation in groundwater by hydrogenotrophic denitrification. *Front. Microbiol.* 12, 443. doi: 10.3389/fmicb.2021.610437
- EPA, U. (2011). *40 CFR APPENDIX b TO PART 136 - DEFINITION AND PROCEDURE FOR THE DETERMINATION OF THE METHOD DETECTION LIMIT-REVISION 1.11* (Washington, DC: U.S. Government Publishing Office).
- Felix, J. D., and Murgulet, D. (2020). Nitrate isotopic composition of sequential hurricane Harvey wet deposition: low latitude NO_x sources and oxidation chemistry. *Atmospheric Environ.* 238, 117748. doi: 10.1016/j.atmosenv.2020.117748
- Findlay, S. E., and Sinsabaugh, R. L. (2004). Aquatic ecosystems: interactivity of dissolved organic matter. *Freshw. Sci.* 23 (3), 662–663. doi: 10.1899/0887-3593(2004)023<0662:AEIODO>2.0.CO;2
- Fritz, A., and Samenow, J. (2017). *Harvey Unloaded 33 trillion gallons of water in the US* (Washington, DC: The Washington Post 2).
- Gardner, W. S., McCarthy, M. J., An, S., Sobolev, D., Sell, K. S., and Brock, D. (2006). Nitrogen fixation and dissimilatory nitrate reduction to ammonium (DNRA) support nitrogen dynamics in Texas estuaries. *Limnology Oceanography* 51 (1part2), 558–568. doi: 10.4319/lo.2006.51.1_part_2.0558
- Gardner, W. S., and Stephens, J. A. (1978). Stability and composition of terrestrially derived dissolved organic nitrogen in continental shelf surface waters. *Mar. Chem.* 6 (4), 335–342. doi: 10.1016/0304-4203(78)90014-2
- Giblin, A. E., Tobias, C. R., Song, B., Weston, N., Banta, G. T., and H. RIVERA-MONROY, V. (2013). The importance of dissimilatory nitrate reduction to ammonium (DNRA) in the nitrogen cycle of coastal ecosystems. *Oceanography* 26 (3), 124–131. doi: 10.5670/oceanog.2013.54
- Glombitza, C., Adhikari, R. R., Riedinger, N., Gilhooly, W. P., Hinrichs, K.-U., and Inagaki, F. (2016). Microbial sulfate reduction potential in coal-bearing sediments down to ~2.5 km below the seafloor off shimokita peninsula, Japan. *Front. Microbiol.* 7. doi: 10.3389/fmicb.2016.01576
- Goff, J. A., Swartz, J. M., Gulick, S. P., Dawson, C. N., and de Alegria-Arzaburu, A. R. (2019). An outflow event on the left side of hurricane Harvey: Erosion of barrier sand and seaward transport through aransas pass, Texas. *Geomorphology* 334, 44–57. doi: 10.1016/j.geomorph.2019.02.038
- Gold-Bouchot, G., Polis, S., Castañón, L. E., Flores, M. P., Alsante, A. N., and Thornton, D. C. O. (2021). Chromophoric dissolved organic matter (CDOM) in a subtropical estuary (Galveston bay, USA) and the impact of hurricane Harvey. *Environ. Sci. Pollut. Res.* 28 (38), 53045–53057. doi: 10.1007/s11356-021-14509-x
- Graham, A. M., Cameron-Burr, K. T., Hajic, H. A., Lee, C., Msekela, D., and Gilmour, C. C. (2017). Sulfurization of dissolved organic matter increases Hg-sulfide-dissolved organic matter bioavailability to a Hg-methylating bacterium. *Environ. Sci. Technol.* 51 (16), 9080–9088. doi: 10.1021/acs.est.7b02781
- Griffith, D. R., and Raymond, P. A. (2011). Multiple-source heterotrophy fueled by aged organic carbon in an urbanized estuary. *Mar. Chem.* 124 (1–4), 14–22. doi: 10.1016/j.marchem.2010.11.003
- Hansell, D., and Carlson, C. (2015). *Biogeochemistry of marine dissolved organic matter, biogeochemistry of marine dissolved organic matter* (Amsterdam, Netherlands: Elsevier). doi: 10.1016/C2012-0-02714-7
- Hauke, J., and Kossowski, T. (2011). Comparison of values of pearson's and spearman's correlation coefficients on the same sets of data. *Quaestiones geographicae* 30 (2), 87–93. doi: 10.2478/v10117-011-0021-1
- Hedges, J. I., and Keil, R. G. (1999). Organic geochemical perspectives on estuarine processes: sorption reactions and consequences. *Mar. Chem.* 65 (1–2), 55–65. doi: 10.1016/S0304-4203(99)00010-9
- Inamdar, S., Singh, S., Dutta, S., Levia, D., Mitchell, M., Scott, D., et al. (2011). Fluorescence characteristics and sources of dissolved organic matter for stream water during storm events in a forested mid-Atlantic watershed. *J. Geophysical Research: Biogeosciences* 116 (G3), 23. doi: 10.1029/2011JG001735
- Kennedy, C. D., Genereux, D. P., Corbett, D. R., and Mitasova, H. (2009). Relationships among groundwater age, denitrification, and the coupled groundwater and nitrogen fluxes through a streambed. *Water Resour. Res.* 45 (9). doi: 10.1029/2008WR007400
- Kim, G., and Hwang, D. W. (2002). Tidal pumping of groundwater into the coastal ocean revealed from submarine 222Rn and CH₄ monitoring. *Geophysical Res. Lett.* 29 (14), 23–21–23-24. doi: 10.1029/2002GL015093
- Koch, B. P., and Dittmar, T. (2006). From mass to structure: An aromaticity index for high-resolution mass data of natural organic matter. *Rapid Commun. mass spectrometry* 20 (5), 926–932. doi: 10.1002/rcm.2386
- Ksionzek, K. B., Zhang, J., Ludwichowski, K.-U., Wilhelms-Dick, D., Trimborn, S., Jendrossek, T., et al. (2018). Stoichiometry, polarity, and organometallics in solid-phase extracted dissolved organic matter of the Elbe-weser estuary. *PLoS One* 13 (9), e0203260. doi: 10.1371/journal.pone.0203260
- Lau, M. P., and Del Giorgio, P. (2020). Reactivity, fate and functional roles of dissolved organic matter in anoxic inland waters. *Biol. Lett.* 16 (2), 20190694. doi: 10.1098/rsbl.2019.0694
- Lee, S.-A., Kim, T.-H., and Kim, G. (2020). Tracing terrestrial versus marine sources of dissolved organic carbon in a coastal bay using stable carbon isotopes. *Biogeosciences* 17 (1), 135–144. doi: 10.5194/bg-17-135-2020
- Letourneau, M. L., and Medeiros, P. M. (2019). Dissolved organic matter composition in a marsh-dominated estuary: Response to seasonal forcing and to the passage of a hurricane. *J. Geophysical Research: Biogeosciences* 124 (6), 1545–1559. doi: 10.1029/2018JG004982
- Li, S., Jiang, Z., and Ji, G. (2022). Effect of sulfur sources on the competition between denitrification and DNRA. *Environ. pollut.* 305, 119322. doi: 10.1016/j.envpol.2022.119322
- Liu, M., Chen, J., Sun, X., Hu, Z., and Fan, D. (2019). Accumulation and transformation of heavy metals in surface sediments from the Yangtze river estuary to the East China Sea shelf. *Environ. pollut.* 245, 111–121. doi: 10.1016/j.envpol.2018.10.128
- Lopez, C. V., Murgulet, D., and Santos, I. R. (2020). Radioactive and stable isotope measurements reveal saline submarine groundwater discharge in a semiarid estuary. *J. Hydrology* 590, 125395. doi: 10.1016/j.jhydrol.2020.125395
- Lu, K., and Liu, Z. (2019). Molecular level analysis reveals changes in chemical composition of dissolved organic matter from south Texas rivers after high flow events. *Front. Mar. Sci.* 6, 673. doi: 10.3389/fmars.2019.00673
- Mallin, M. A., Posey, M. H., Shank, G. C., McIver, M. R., Ensign, S. H., and Alphin, T. D. (1999). Hurricane effects on water quality and benthos in the cape fear watershed: natural and anthropogenic impacts. *Ecol. Appl.* 9 (1), 350–362. doi: 10.1890/1051-0761(1999)009[0350:HEOWQA]2.0.CO;2
- McKenzie, T., Dulai, H., and Fuleky, P. (2021). Traditional and novel time-series approaches reveal submarine groundwater discharge dynamics under baseline and extreme event conditions. *Sci. Rep.* 11 (1), 1–14. doi: 10.1038/s41598-021-01920-0
- Montagna, P., Palmer, T. A., and Pollack, J. B. (2012). *Hydrological changes and estuarine dynamics* (Springer Science & Business Media).
- Moosdorf, N., Böttcher, M. E., Adyasar, D., Erkul, E., Gilfedder, B. S., Greskowiak, J., et al. (2021). A state-of-the-art perspective on the characterization of subterranean estuaries at the regional scale. *Front. Earth Sci.* 9, 95. doi: 10.3389/feart.2021.601293
- Morton, R. A., and Winker, C. D. (1979). *Distribution and significance of coarse biogenic and clastic deposits on the Texas inner shelf (1)*. Gulf Coast Association of Geological Societies Transactions, 29, 306–320
- Murgulet, D., Lopez, C. V., and Douglas, A. R. (2022). Radioactive and stable isotopes reveal variations in nearshore submarine groundwater discharge composition and magnitude across low inflow northwestern gulf of Mexico estuaries. *Sci. Total Environ.* 823, 153814. doi: 10.1016/j.scitotenv.2022.153814
- Murgulet, D., Murgulet, V., Spalt, N., Douglas, A., and Hay, R. G. (2016). Impact of hydrological alterations on river-groundwater exchange and water quality in a semi-arid area: Nueces river, Texas. *Sci. Total Environ.* 572, 595–607. doi: 10.1016/j.scitotenv.2016.07.198
- Murgulet, D., Trevino, M., Douglas, A., Spalt, N., Hu, X., and Murgulet, V. (2018). Temporal and spatial fluctuations of groundwater-derived alkalinity fluxes to a semiarid coastal embayment. *Sci. Total Environ.* 630, 1343–1359. doi: 10.1016/j.scitotenv.2018.02.333
- NOAA (2017). *National hurricane center*.
- Ohno, T., Sleighter, R. L., and Hatcher, P. G. (2016). Comparative study of organic matter chemical characterization using negative and positive mode electrospray ionization ultrahigh-resolution mass spectrometry. *Analytical bioanalytical Chem.* 408 (10), 2497–2504. doi: 10.1007/s00216-016-9346-x
- Opsahl, S., and Benner, R. (1997). Distribution and cycling of terrigenous dissolved organic matter in the ocean. *Nature* 386 (6624), 480–482. doi: 10.1038/386480a0
- Paerl, H. W., Pinckney, J. L., Fear, J. M., and Peierls, B. L. (1998). Ecosystem responses to internal and watershed organic matter loading: consequences for hypoxia in the eutrophying neuse river estuary, north Carolina, USA. *Mar. Ecol. Prog. Ser.* 166, 17–25. doi: 10.3354/meps166017
- Raymond, P. A., and Saiers, J. E. (2010). Event controlled DOC export from forested watersheds. *Biogeochemistry* 100 (1–3), 197–209. doi: 10.1007/s10533-010-9416-7
- Riera, P., Montagna, P., Kalke, R., and Richard, P. (2000). Utilization of estuarine organic matter during growth and migration by juvenile brown shrimp penaeus aztecus in a south Texas estuary. *Mar. Ecol. Prog. Ser.* 199, 205–216. doi: 10.3354/meps199205

- Santos, I. R., Burnett, W. C., Dittmar, T., Suryaputra, I. G., and Chanton, J. (2009). Tidal pumping drives nutrient and dissolved organic matter dynamics in a gulf of Mexico subterranean estuary. *Geochimica Cosmochimica Acta* 73 (5), 1325–1339. doi: 10.1016/j.gca.2008.11.029
- Santos, L., Pinto, A., Filipe, O., Cunha, A., Santos, E. B., and Almeida, A. (2016). Insights on the optical properties of estuarine DOM—hydrological and biological influences. *PLoS One* 11 (5), e0154519. doi: 10.1371/journal.pone.0154519
- Savage, C., Thrush, S. F., Lohrer, A. M., and Hewitt, J. E. (2012). Ecosystem services transcend boundaries: estuaries provide resource subsidies and influence functional diversity in coastal benthic communities. *PLoS One* 7 (8), e42708. doi: 10.1371/journal.pone.0042708
- Schafer, T., Ward, N., Julian, P., Reddy, K. R., and Osborne, T. Z. (2020). Impacts of hurricane disturbance on water quality across the aquatic continuum of a blackwater river to estuary complex. *J. Mar. Sci. Eng.* 8 (6), 412. doi: 10.3390/jmse8060412
- Schmidt, F., Elvert, M., Koch, B. P., Witt, M., and Hinrichs, K.-U. (2009). Molecular characterization of dissolved organic matter in pore water of continental shelf sediments. *Geochimica Cosmochimica Acta* 73 (11), 3337–3358. doi: 10.1016/j.gca.2009.03.008
- Schmidt, F., Koch, B. P., Goldammer, T., Elvert, M., Witt, M., Lin, Y.-S., et al. (2017). Unraveling signatures of biogeochemical processes and the depositional setting in the molecular composition of pore water DOM across different marine environments. *Geochimica Cosmochimica Acta* 207, 57–80. doi: 10.1016/j.gca.2017.03.005
- Seitzinger, S., and Sanders, R. (1999). Atmospheric inputs of dissolved organic nitrogen stimulate estuarine bacteria and phytoplankton. *Limnology Oceanography* 44 (3), 721–730. doi: 10.4319/lo.1999.44.3.0721
- Seitzinger, S. P., Sanders, R., and Styles, R. (2002). Bioavailability of DON from natural and anthropogenic sources to estuarine plankton. *Limnology Oceanography* 47 (2), 353–366. doi: 10.4319/lo.2002.47.2.0353
- Shang, P., Lu, Y., Du, Y., Jaffé, R., Findlay, R. H., and Wynn, A. (2018). Climatic and watershed controls of dissolved organic matter variation in streams across a gradient of agricultural land use. *Sci. Total Environ.* 612, 1442–1453. doi: 10.1016/j.scitotenv.2017.08.322
- Sharma, V., Rhudy, K., Koenig, R., Baggett, A., Hollyfield, S., and Vazquez, F. (1999). Metals in sediments of Texas estuaries, USA. *J. Environ. Sci. Health Part A* 34 (10), 2061–2073. doi: 10.1080/10934529909376947
- Shelton, M. L. (2009). *Hydroclimatology: perspectives and applications* (Cambridge, UK: Cambridge University Press).
- Singh, S., Dash, P., Sankar, M., Silwal, S., Lu, Y., Shang, P., et al. (2019). Hydrological and biogeochemical controls of seasonality in dissolved organic matter delivery to a blackwater estuary. *Estuaries Coasts* 42 (2), 439–454. doi: 10.1007/s12237-018-0473-9
- Sipler, R. E., and Bronk, D. A. (2015). “Dynamics of dissolved organic nitrogen,” in *Biogeochemistry of marine dissolved organic matter*, (London: Academic Press), 2nd Edition, 127–232.
- Sleighter, R. L., Liu, Z., Xue, J., and Hatcher, P. G. (2010). Multivariate statistical approaches for the characterization of dissolved organic matter analyzed by ultrahigh resolution mass spectrometry. *Environ. Sci. Technol.* 44 (19), 7576–7582. doi: 10.1021/es1002204
- Smith, M. A., Kominoski, J. S., Gaiser, E. E., Price, R. M., and Troxler, T. G. (2021). Stormwater runoff and tidal flooding transform dissolved organic matter composition and increase bioavailability in urban coastal ecosystems. *J. Geophysical Research: Biogeosciences* 126 (7), e2020JG006146. doi: 10.1029/2020JG006146
- So, S., Juarez, B., Valle-Levinson, A., and Gillin, M. E. (2019). Storm surge from hurricane Irma along the Florida peninsula. *Estuarine Coast. Shelf Sci.* 229, 106402. doi: 10.1016/j.ecss.2019.106402
- Stearns, J. (2019). SEG technical program expanded abstracts. *Soc. Explor. Geophysicists.*, 2780–2786. doi: 10.1190/segam2019-3216805.1
- Steichen, J. L., Labonté, J. M., Windham, R., Hala, D., Kaiser, K., Setta, S., et al. (2020). Microbial, physical, and chemical changes in Galveston bay following an extreme flooding event, hurricane Harvey. *Front. Mar. Sci.* 7, 186. doi: 10.3389/fmars.2020.00186
- Sun, J., Khan, E., Simsek, S., Ohm, J.-B., and Simsek, H. (2017). Bioavailability of dissolved organic nitrogen (DON) in wastewaters from animal feedlots and storage lagoons. *Chemosphere* 186, 695–701. doi: 10.1016/j.chemosphere.2017.07.153
- Taniguchi, M., and Iwakawa, H. (2004). Submarine groundwater discharge in Osaka bay, Japan. *Limnology* 5 (1), 25–32. doi: 10.1007/s10201-003-0112-3
- Traving, S. J., Rowe, O., Jakobsen, N. M., Sørensen, H., Dinasquet, J., Stedmon, C. A., et al. (2017). The effect of increased loads of dissolved organic matter on estuarine microbial community composition and function. *Front. Microbiol.* 8, 351. doi: 10.3389/fmicb.2017.00351
- TWDB (2020). *Water for Texas, lake evaporation and precipitation*. Texas Water Development Board. Available at: <https://waterdatafortexas.org/lake-evaporation-rainfall> (Accessed January 2020)
- Webster, P. J., Holland, G. J., Curry, J. A., and Chang, H.-R. (2005). Changes in tropical cyclone number, duration, and intensity in a warming environment. *Science* 309 (5742), 1844–1846. doi: 10.1126/science.1116448
- Wong, W. W., Applegate, A., Poh, S. C., and Cook, P. L. (2020). Biogeochemical attenuation of nitrate in a sandy subterranean estuary: Insights from two stable isotope approaches. *Limnology Oceanography* 65 (12), 3098–3113. doi: 10.1002/lno.11576
- Yan, G., Labonté, J. M., Quigg, A., and Kaiser, K. (2020). Hurricanes accelerate dissolved organic carbon cycling in coastal ecosystems. *Front. Mar. Sci.* 248. doi: 10.3389/fmars.2020.00248